A tectorin-based matrix and planar-cell-polarity genes are required for normal collagen-fibril orientation in the developing tectorial membrane

Article (Accepted Version)

A TECTORIN-BASED MATRIX AND PLANAR-CELL-POLARITY GENES ARE REQUIRED FOR NORMAL COLLAGEN-FIBRIL ORIENTATION IN THE DEVELOPING TECTORIAL MEMBRANE

Richard J. Goodyear[1], Xiaowei Lu[2], Michael R. Deans[3,4] and Guy P. Richardson[1]

[1]Sussex Neuroscience, School of Life Sciences, University of Sussex, Brighton, BN1 9QG, UK
[2]Department of Cell Biology, University of Virginia Health System, Charlottesville, VA 22098, USA
[3]Department of Surgery, Division of Otolaryngology, University of Utah School of Medicine, Salt Lake City, UT, USA
[4]Department of Neurobiology & Anatomy, University of Utah School of Medicine, Salt Lake City, UT, USA

Summary: This paper shows collagen-fibril orientation in the developing tectorial membrane of the cochlea depends on both a tectorin-based matrix and normal expression patterns of planar-cell-polarity in the underlying epithelium.

List of abbreviations: Tectorial membrane, TM; Outer hair cell, OHC; Inner hair cell, IHC; Greater epithelial ridge, GER; Planar cell polarity, PCP; Embryonic day, E; Postnatal day, P; Transmission electron microscopy, TEM; Scanning electron microscopy, SEM; Horse serum, HS; Phosphate buffered saline, PBS; Triton X-100, TX; Enhanced green fluorescent protein, EGFP.

Abstract

The tectorial membrane is an extracellular structure of the cochlea. It develops on the surface of an epithelium and contains collagen fibrils embedded in a tectorin-based matrix. The collagen fibrils are oriented radially with an apically-directed slant - a feature considered critical for hearing. To determine how this pattern is generated, collagen-fibril formation was examined in mice lacking a tectorin-based matrix, epithelial cilia, or the planar-cell-polarity genes *Vangl2* and *Ptk7*. In wild-type mice, collagen-fibril bundles appear within a tectorin-based matrix at E15.5 and, as fibril-number rapidly increases, become co-aligned and correctly oriented. Epithelial-width measurements and data from *Kif3a*^{cKO} mice suggest, respectively, radial stretch and cilia play little, if any, role in determining normal collagen-fibril orientation, but evidence from tectorin-knockout mice indicates confinement is important. PRICKLE2 distribution reveals the planar-cell-polarity axis in the underlying epithelium is organised along the length of the cochlea and, in mice in which this polarity is disrupted, the apically-directed collagen offset is no longer observed. These results highlight the importance of the tectorin-based matrix and epithelial signals for precise collagen organisation in the tectorial membrane.

Introduction

The tectorial membrane (TM) is an extracellular structure that spirals along the length of the cochlea, and lies over the organ of Corti (Fig. 1A). It attaches medially to the spiral limbus, stretches over the spiral sulcus, and connects laterally to the hair bundles of the outer hair cells (OHCs), the cells that amplify the motion of the basilar membrane at low sound pressure levels (Ashmore, 2008; Dallos, 2008). Once thought to act as a rigid plate that hinged around its point of limbal attachment (Davis, 1965), the TM is now known to play a more complex role (Lukashkin et al., 2010). It acts as an inertial mass against which the OHCs can react, thereby regulating the amplification of basilar membrane motion (Gummer et al., 1996; Legan et al., 2000), and it modulates fluid flow in the sub-tectorial space, driving the inner hair cells (IHCs) optimally at their best frequency (Nowotny and Gummer, 2006; Legan et al., 2005). The TM also supports travelling waves that couple OHCs along the length of the cochlea, therefore determining the sharpness of cochlear tuning (Russell et al., 2007; Ghaffari et al., 2010; Meaud and Grosh, 2010).

The TM is composed of collagens typically found in cartilage (Types II, V, IX and XI) and a set of non-collagenous glycoproteins that are only expressed at high levels in the inner ear (TECTA, TECTB, CEACAM16, OTOGELIN and OTOGELIN-LIKE) (Richardson et al., 1987; Thalmann, 1993; Legan et al., 1997; Zheng et al., 2011; Cohen-Salmon et al., 1997; Yariz et al., 2012). The collagens form bundles of 20 nm-diameter fibrils that are arrayed across the width of the TM with a slight offset towards the apical end of the cochlea, hereafter referred to as a near-radial orientation (Fig. 1B). This offset increases from ~15^{o} in basal regions to 25^{o} at the apex in the region overlying the hair bundles (Fig. 1C) (Lim, 1972). TECTA, TECTB and CEACAM16 are major components of the striated-sheet matrix within which the collagen fibrils are imbedded (Hasko and Richardson, 1988; Legan et al., 2000; Russell et al., 2007; Zheng et al., 2011; Kammerer et al., 2012), and are also associated with other structures, including the marginal band, the covernet fibrils and Hensen's stripe, peripheral features that run principally along the length of the TM (FIG. 1A-B).

The TM forms on the luminal surface of the developing cochlear duct of the mouse over a period of ~25 days, between embryonic day (E) 12 and postnatal day (P) 16. It is produced by the cells of the greater and lesser epithelial ridges (Lim, 1987), regions in the ventral wall of the duct that eventually give rise to the spiral limbus, the spiral sulcus, and the organ of Corti (Kelley, 2007). In this study we address when and how the collagen fibrils become oriented across the width of the TM and become aligned along the OHCs' axis of mechanosensitivity. Such an arrangement generates mechanical anisotropy, and is thought

to ensure forces are delivered optimally from the hair bundles of the OHCs to those of the IHCs (Gavara and Chadwick, 2009).

Using wild-type mice and mice with mutations in a number of genes, we provide evidence that the initial alignment and orientation of the collagen fibrils in the TM occurs rapidly and before a significant radial expansion of the cochlear epithelium. It also occurs in the absence of apically-located epithelial cilia but is critically dependent on the presence of the tectorin-based matrix. The latter may initially confine and align the collagen fibrils radially as they polymerise, and then allow further polymerisation to occur without influence from the forces generated by the longitudinal extension of the epithelium. Fine tuning of collagen-fibril orientation is, however, dependent on the cellular organisation of the epithelium as loss-of-function mutations in planar-cell-polarity genes that disrupt PRICKLE2 distribution in the cells of the greater epithelial ridge (GER) have distinct effects on collagen patterning.

Methods

Animals

CD1 mice were used to study TM-development in wild-type mice. Cochleae were obtained from embryos derived from timed-mated females at E14.5 (n=10), E15.5 (n=29), E16.5 (n=15) and E17.5 (n=6). Cochleae were also obtained from pups at P1 (n=8), P3 (n=7) and P5 (n=4). Additional CD1 cochleae were used for transmission electron microscopy (TEM) at E14.5 (n=4), E15.5 (n=4), E16.5 (n=3) and E17.5 (n=3). Cochleae from *Tecta/b*^{dKO} mice (see below) were obtained at E15.5 (n=35), E16.5 (n=31), E17.5 (n=19), P1 (n=7), P3 (n=5), P5 (n=5) and P10 (n=3). Cochleae from mice doubly heterozygous for the *Tecta/b* null mutations were obtained at E15.5 (n=9), E16.5 (n=9) and E17.5 (n=7) from crosses set up between *Tecta/b*^{dKO} mice and CD1 mice. *Foxg1*-Cre; *Kif3a*$^{flox/flox}$ (*Kif3a*^{cKO}) cochleae were used at E18.5 (mutant n=6; control n=4) and E16.5 (mutant n=2; control n=3). *Pax2*-Cre; *Vangl2*$^{flox/flox}$ (*Vangl2*^{cKO}) cochleae were used at E17.5 and P1 for COL9A staining (P1: mutant n=3, control n=3; E17.5 mutant n=8, control =8) and at P1-2 for PRICKLE2 staining (mutant n=3, control n=3). *Pax2*-Cre; *Ptk7*$^{flox/flox}$ (*Ptk7*^{cKO}) cochleae were used at P1 and P6 for COL9A staining (P1: mutant n=4, control n=3; P6: mutant n=4, control n=3) and at P1 for PRICKLE2 staining (mutant n=4; control n=3); *Ptk7*$^{-/-}$ (*Ptk7*^{KO}) cochleae were used at E16.5-E17.5 for scanning electron microscopy (mutant n=4; control n=4) and COL9A staining (mutant n=4; control n=3). Mice of either sex were used and n numbers refer to numbers of animals. Animal procedures were carried out under UK Home Office Project licence (PPL70/7658) with approval of the local Animal Welfare and Ethical Review Board at the

University of Sussex, and in compliance with NIH guidelines and approval of the local Animal Care and Use committees at the Universities of Utah and Virginia.

Transgenic mouse production

Production of an EGFP knockin-*Tecta* knockout mouse (*Tecta*$^{EFGP/EGFP}$ mouse) in which an EGFP minigene was inserted into the first coding exon of *Tecta* is to be described elsewhere. The mouse expresses EGFP from the *Tecta* locus in the cells of the developing cochlea from E13.5 to P7 (RJG and GPR, unpublished). TECTA cannot be detected in the *Tecta*$^{EGfP/EGFP}$ cochlea using immunofluorescence microscopy with polyclonal antibody R9 (Knipper et al., 2001) and a TM is no longer present on the organ of Corti in mature animals, as described previously for a *Tecta* functional-null mutant mouse (the *Tecta*^{tm1Gpr} or *Tecta*$^{\Delta ENT}$ mouse; Legan et al., 2000). A *Tecta/Tectb* double-null mutant (double knockout) mouse was created by crossing the *Tecta*$^{EFGP/EGFP}$ mouse with a *Tectb*$^{-/-}$ mouse (*Tectb*^{tm1Gpr} ; Russell et al., 2007). The resultant mice, doubly heterozygous at both loci, were inbred to produce *Tecta*$^{EGFP/EGFP}$, *Tectb*$^{-/-}$ mice that were maintained as an inbred colony. These mice will be referred to as *Tecta/b* double knockout (*Tecta/b*^{dKO}) mice and are on a mixed, variable S129SvEv/C57Bl6J background.

Fixation and tissue preparation for light microscopy

Cochleae were fixed in 3.7% (v/v) formaldehyde in 0.1 M sodium phosphate pH 7.4 for 1-3 hours, and washed in phosphate buffered saline (PBS). The otic capsule and the ventral wall of the cochlea were removed prior to staining wholemount preparations. For COL9A (Collagen IX) or TECTA (α-tectorin) staining, samples were pre-blocked in PBS containing 10% heat-inactivated horse serum (PBS/HS) for 1 hour and then incubated overnight in rabbit anti-pig COL9A (a gift from Prof. A Bailey and Dr. V Duance, AFRC, Bristol, UK) or rabbit anti-chick TECTA (R9; Knipper et al., 2001). Both sera were used at a dilution of 1:1000. For anti-EGFP staining, samples were pre-blocked in PBS/HS containing 0.1% Triton X-100 (PBS/HS/TX) for one hour, and then incubated overnight in FITC-conjugated goat anti-EGFP antibody (ab6662, Abcam) at a dilution of 1:1000. Anti-acetylated tubulin IgG2b clone 6-11B-1 (Sigma-Aldrich) was used at 1:500 overnight in PBS/HS/TX followed by Alexa-555 conjugated goat anti-IgG2b. Affinity-purified rabbit anti-PRICKLE2 antibody (Deans et al., 2007) was used at 1:250 overnight in PBS/HS/TX. All Alexa-conjugated secondary antibodies (Invitrogen) were used at 1:500 for 2-3 hours. Phalloidin staining of PBS/HS/TX-permeabilised samples was carried out with either TRITC-conjugated phalloidin (Sigma-Aldrich, 0.1 µg/ml) or Alexa-633 conjugated phalloidin (Invitrogen, 1:100) for at least

2-3 hours. Overnight incubations were carried out at 4°C, all other steps were performed at room temperature. Following labelling, samples were washed 3x in PBS and mounted in Vectashield (Vector Laboratories) with or without supporting shims created by stacking plastic self-adhesive washers on the slide (Fisher Clark). In some cases, TMs were obtained by dissection and processed in a similar manner. Cryosections of formaldehyde-fixed cochleae were stained overnight with rabbit antibodies to chick TECTA (R9), chick-TECTB (R7; Knipper et al., 2001), recombinant fragments of mouse otogelin (Cohen-Salmon et al., 1997) or Col9A (Duance et al., 1982) at a dilution of 1:1000, followed by Alexa-488 goat and rabbit IgG (1:500) and Texas-Red conjugated phalloidin (1:300). Samples were imaged on Zeiss LSM 510 or Leica SP8 confocal microscopes or on a Zeiss Axioplan-2 wide-field fluorescence microscope. Further image analysis was performed with LSM Image Browser (Zeiss), ImageJ (NIH) and Photoshop CS5 (Adobe).

Fixation and tissue preparation for transmission electron microscopy

Labyrinths were separated from the skull, the stapes removed and the cochlear windows opened to improve fixative penetration. Cochleae were fixed in 2.5% glutaraldehyde in 0.1 M sodium cacodylate pH 7.4 containing 1% (w/v) tannic acid (ACS grade, Sigma-Aldrich) for 3-4 hours, washed in 0.1 M sodium cacodylate buffer, post-fixed in 1% osmium tetroxide in the same buffer for 2 hours, washed 3x in buffer, once in water and dehydrated through an ascending ethanol series. After equilibrating in propylene oxide, samples were embedded in Epon resin, cured at 60°C for 24h and sectioned with a diamond knife on a Reichert-Jung Ultracut E ultramicrotome at 80-90 nm thickness to obtain cross-sections of the TM in the apical and basal coils. Sections were collected on copper-mesh grids, stained with uranyl acetate and lead citrate and viewed in a Hitachi 7100 transmission electron microscope. Images were captured with a Gatan Ultrascan 1000 camera.

Fixation and tissue preparation for scanning electron microscopy

Labyrinths were separated from the skull, the stapes removed and the cochlear windows opened up. Cochleae were fixed in 2.5% glutaraldehyde in 0.1 M sodium cacodylate pH 7.4 for 2-3 hours, washed 3x in 0.1 M sodium cacodylate buffer, and the lateral wall removed to reveal the TM. Tissues were post-fixed with 1% osmium tetroxide in 0.1 M sodium cacodylate buffer for 2-3 hours, dehydrated through ascending concentrations of ethanol, critical point-dried, mounted on support stubs and sputter-coated with platinum. Samples were imaged with a Jeol 6700F SEM.

Cochlear length and width measurements at E15.5-E17.5

For measuring the length of the developing organ of Corti, cochleae were stained to amplify the EGFP signal (heterozygous *Tecta/b*^{dKO} mice) or labelled with phalloidin (all cochleae), and imaged using a x10 objective. The images were photo-montaged using Photoshop CS5 and measurements were made at the location of the IHCs using ImageJ. For width measurements, confocal z-stacks were oriented in ImageJ such that an orthogonal slice could be taken perpendicular to the long axis of the cochlea, at defined points from the basal-most end. These points were at intervals of 10 IHCs counting from the basal end, from IHC-10 to IHC-110. The width of the EGFP-positive epithelium at these points was measured at its surface from these orthogonal images, with measurements being made from the medial-most edge of the EGFP staining to the medial edge of the IHC.

Measurements of cell numbers

Measurements of cell numbers in regions of the GER underlying the TM were acquired in boxes 50 microns wide (in the apical-basal axis) by 100 microns in depth (the medio-lateral axis) with the box positioned just medial to the IHC surfaces. Cells were scored as being within the box in phalloidin-stained preparations if their apical surface was entirely within the boundary of the box or if it intersected the lower or left-side boundary edges.

Antibody validation

Antibodies raised to the a-1 fragment of chicken TECTA and chicken TECTB (Knipper et al., 2001) specifically stain the TM in cryosections of the mouse cochlea but do not stain in the respective null-mutant mice, the EGFP knockin-*Tecta* knockout mouse (unpublished observations) and the *Tectb*$^{-/-}$ mouse (Russell et al., 2007). COL9A antibody specifically stains bands of the expected size on western blots of the mouse TM and shows no cross-reactivity with either Type II or Type XI collagen (Richardson et al., 1987). Antibodies to recombinant fragments of OTOGELIN (Cohen-Salmon et al., 1997) were prepared and purified commercially (Eurogentec). PRICKLE2 antibody was validated as described previously (Deans et al., 2007).

Results

A tectorin-based matrix precedes the appearance of collagen fibrils

Immunofluorescence microscopy was used to compare the distribution and appearance of the collagenous and non-collagenous components of the TM during its early development (Figure 2). TECTA and TECTB are readily detected at E14.5 (Fig. 2 A, B), but OTOG levels are very low relative to those seen in the overlying epithelium (Fig. 2C) and COL9A staining cannot be observed (Fig. 2D). By E15.5, the level of OTOG staining within the TM increases (Fig. 2G), and COL9A immunoreactivity appears as a fine layer lying within its central core (Fig. 2H). By E16.5, the TM is considerably thicker and labels strongly for all four proteins (Fig. 2I-L). Whilst TECTA is distributed uniformly throughout the TM at E16.5 (Fig. 2I), TECTB and OTOG are concentrated on the upper surface (Fig. 2J, K) and COL9A is confined to the central region (Fig. 2L).

Radially-aligned collagen fibrils form within a 24 hour time frame

Electron microscopy (Figure 3) was used to examine these early stages of TM development in further detail, with a focus on the basal high-frequency region of the cochlea that is known to mature first. At E14.5 the TM is formed from an upper layer of densely-packed filaments that are organised into cords and run in a longitudinal direction, and a lower layer of loosely-packed filamentous material (Fig. 3A, B). Collagen fibrils are not observed in the TM at this stage (Fig. 3B), corroborating the data obtained with immunofluorescence microscopy (see above, Fig. 2D). By E15.5, the depth of the TM is greater, the upper layer has increased in density, and collagen fibrils with a characteristic diameter of 20 nm are present (Fig. 3C). These fibrils lie predominantly within the lower layer of the TM, are largely located above and not between the microvilli of the underlying epithelial cells, and are loosely associated into bundles that have an apparently random organisation (Fig. 3C). At E16.5, the TM has further increased in depth, the upper dense layer is more substantial than at earlier stages, and the collagen-fibril bundles have a radial orientation (Fig. 3D). In developing cartilage, collagen fibrils are aligned by fibripositors, myosin II driven recesses in the plasma membranes of the surrounding fibroblasts (Canty et al., 2004; Kapacee et al., 2008; Kalson et al., 2013). A careful examination of the apical domain of the epithelial cells of the GER, however, failed to provide evidence for the presence of such recesses or similar structures at these or later stages of development.

Whole-mount preparations of cochleae were double-labelled with phalloidin and antibodies to COL9A to examine closely the changes occurring in collagen fibril-bundle organisation between E15.5 and E16.5 (Figure 4). Confocal projections confirm that the first collagen-fibril bundles to appear at E15.5 are, as expected from the electron microscopy, randomly oriented (Fig. 4 A, B). A comparison of equivalent regions of the cochlea at E15.5 and E16.5 reveals there is a marked increase in collagen-fibril bundle density by E16.5 (Fig. 4 D, E), with the fibrils adopting a highly-organised, near-radial pattern. This arrangement largely resembles that seen in the mature animal, and includes the characteristic offset of the fibrils toward the apex of the cochlea.

Radial alignment of collagen fibrils can occur without medio-lateral expansion of the underlying epithelium

With solutions of collagen that are allowed to polymerise in the absence of cells *in vitro*, imposed strain (Vader et al., 2009), molecular crowding/confinement (Saeidi et al., 2012) and fluid flow (Lee et al., 2006) are all able to produce aligned collagen fibrils. Phalloidin staining reveals there is an increase in the surface area of the apical profiles of cells in the medial zone of the GER between E15.5 (Fig. 4C) and E16.5 (Fig. 4F) and suggests an expansion in the width of the epithelium underlying the TM may generate the radial patterning of collagen-fibril bundles. *Tecta*^{EGFP} mice were therefore used to examine changes in the dimensions of this region as the collagen fibrils become aligned and oriented (Figure 5A).

Labelling *Tecta*$^{+/EGFP}$ mice with antibodies to TECTA demarcates the boundaries of the TM and shows that it extends across the entire surface of the region defined by the distribution of EGFP+ve GER cells between E15.5 and E17.5 (Fig 5B-D), consistent with the TM expanding in conjunction with growth of the underlying epithelium. The width of this EGFP+ve region (as demarcated by arrows in Fig. 5B-D) was therefore measured from defined points along the length of the basal cochlear duct at E15.5, E16.5 and E17.5. IHCs were counted from the basal end (see Fig. 5A), and orthogonal projections were produced from confocal stacks at regions located 10-110 IHCs from the base, at 10 IHC intervals. Fig. 5 B-D show examples of profiles used, with each corresponding to a point that was 70 IHCs from the basal end of the cochlea. Whilst there is a small, but significant increase (~15%) in the width of the GER in the region spanning IHC60 to IHC110 between E15.5 and E16.5, there is not a significant increase in the basal region (between IHC10 and IHC50) during this period (Fig. 5E), the period over which the collagen fibrils are becoming co-aligned and near-radially oriented. Furthermore, the overall percentage increase in the width of the GER in the

basal region of the cochlea is no greater than the increase in its length that occurs during this time frame (Fig. 5F). A larger (30-40%) increase in the width of the GER occurs between E16.5 and E17.5 at all points measured (Fig. 5E). Although this width increase is proportionally greater than the concomitant increase in cochlear length occurring during this period, both for the entire cochlea (19.7%) and for the basal region (12.1%) analysed (see Fig. 5F), this happens after and not during the initial co-alignment and near-radial orientation of the collagen fibrils.

Collagen fibrils initially fail to orient radially in the absence of a tectorin-based matrix

As the appearance of a non-collagenous, tectorin-based matrix precedes the appearance of collagen fibrils, and as the morphological data presented above indicate the collagen fibrils polymerise and align within this matrix, collagen-fibril development in wild type mice (Fig. 6 A, C, E) was compared with that in the in the *Tecta/b*^{dKO} mouse (Fig. 6 B, D, F), a mouse in which neither TECTA, TECTB nor OTOG cannot be detected (unpublished observations). Unlike those in wild-type mice (Fig. 6A), the collagen fibrils in the *Tecta/b*^{dKO} mouse at E15.5 are compact, of varying diameter and oriented in many directions (Fig. 6B). By E16.5, the collagen-fibril bundles in the *Tecta/b*^{dKO} TM become more substantial but remain, relative to those in the wild type, incorrectly oriented (Fig. 6C, D). Transmission electron microscopy reveals the electron-dense cords that are normally present on the surface of the TM (Fig. 6E) are completely absent the *Tecta/b*^{dKO} mouse (Fig. 6F), and suggests these structures may serve to confine the collagen as it polymerises.

However, and somewhat unexpectedly, although the collagen-fibril bundles that are initially produced in the *Tecta/b*^{dKO} mice by E16.5 are of variable diameter and randomly oriented, by P0 and at later early-postnatal stages the TM of the *Tecta/b*^{dKO} mouse is composed of an upper layer of disorganised, thicker collagen-fibril bundles, similar to those seen at E16.5, and a lower layer comprised of finer-diameter bundles that are remarkably well co-aligned (Fig. 7A-C). Transmission electron microscopy fails to reveal the presence of any dense cords or covernet-like material on the upper surface of the *Tecta/b*^{dKO} TM at these stages, and the aligned collagen-fibril bundles that are seen in the lower layer of the TM are closely opposed by an overlying network of disorganised collagen (Fig. 7D).

Although the lower-layer collagen-fibril bundles seen in the TMs of *Tecta/b*^{dKO} mice at later stages (P0-P3) are co-aligned, they are abnormally offset towards the basal, instead of the apical, end of the organ of Corti (Fig. 8A, B), at least in the higher-frequency regions of the

cochlea. This discrepancy in the offset of the co-aligned collagen fibrils seen in the lower layer of the TM in the *Tecta/b*^{dKO} mice is even more exaggerated at the extreme basal tip of the organ of Corti, a region where, over a distance of ~50 microns, the fibrils of wild-type mice are oriented with a slight basal-ward tilt (Fig. 8C, E). In striking contrast, the collagen fibril-bundles in the lower layer of this region of the TM in the *Tecta/b*^{dKO} cochlea are oriented strictly along the length, instead of the width, of the organ of Corti (Fig. 8D, F). Wholemount preparations of the entire *Tecta/b*^{dKO} TM stained with anti-COL9A (Fig. 8G) indicate that the lower-layer collagen-fibril bundles are only abnormally offset in the basal third of the TM. Those in the remaining two thirds have the expected apically-directed slant.

Cilia are not required for the radial alignment of collagen fibrils

Although a tectorin-based matrix is clearly necessary for the formation, co-alignment and orientation of the first collagen fibril bundles that appear within the TM, it is not required for the co-alignment and bundling of the collagen-fibril bundles that form later. The potential roles of other cues were therefore examined. In scanning and transmission electron micrographs, the collagen fibrils of the developing TM that are immediately adjacent to the surface of the GER often appear to be attached to the cilia of the underlying cells (Fig. 9A, B). The possibility that this cilial attachment could be orchestrating the alignment and orientation of collagen fibrils was investigated using a conditional *Kif3a* knockout mouse (*Kif3a*^{cKO}) that lacks cilia within the inner ear (Sipe and Lu, 2011). Confocal images of cochlear ducts taken from heterozygous control (Fig. 10A-C, G) and *Kif3a*^{cKO} (Fig. 10D-F, H) mice at E16.5 and E18.5 reveal that despite an absence of cilia (Fig. 10D-E) and some deformity and shortening of the cochlear duct (not shown), collagen fibril-bundle alignment within the TM is remarkably well maintained (Fig. 10H) in the *Kif3a* knockout mouse.

PCP pathway genes are required for fine tuning collagen fibril orientation

The role of the planar-cell polarity (PCP) genes in establishing the correct orientation of sensory hair bundles in the developing cochlea has been well established (Montcouquiol et al., 2003; Wang et al., 2005; Wang et al., 2006; see also reviews, May-Simera and Kelley, 2012; Ezan and Montcouquiol, 2013; Lu and Sipe, 2016). Interestingly, whilst PRICKLE2 is asymmetrically distributed in inner pillar cells and stains just the medial edge of these cells within the organ of Corti, it is aligned in the orthogonal direction in cells within the GER (Copley et al., 2013). Closer examination of PRICKLE2 distribution in the GER shows it is present in a narrow stripe within the width of the GER that lies approximately beneath the middle of the TM (Fig. 11A-C). PRICKLE2 specifically localises to the apical pole of the cells

in this region, and its distribution defines an axis of planar cell polarity that is broadly directed along the length of the cochlea with little or no staining seen on either the medial or lateral boundaries of these cells. The overall pattern of staining across this stripe gives the appearance of diagonal lines that have an apically-directed slant (arrows in Fig 11). Furthermore, the angle of this slant progressively increases towards the apical end of the cochlea (Fig. 11A-C). This slant resembles that seen in the overlying collagen fibrils (Fig. 12A-B, G-H) in equivalent regions of the cochlea (see Fig.1C).

In *Vangl2*^{cKO} mice, PRICKLE2 is no longer asymmetrically localised and is, instead, distributed equally around the periphery of cells within this GER stripe (Fig. 12C-D'). This loss of asymmetrical PRICKLE2 staining is accompanied by a striking loss in the normal apical slant of collagen-fibril bundles, which instead have an almost strictly-radial orientation (Fig. 12I-J). An identical phenotype is observed following cochlear deletion of another PCP gene, *Ptk7* (Fig. 12E-F, K-L). Whilst these observations provide good evidence that PCP genes can fine tune the orientation of collagen fibrils in then TM, the abnormal basal slant of the collagen fibrils seen in the lower layer of the TM in the basal third of cochlea of the Tecta/bdKO (Fig. 8) does not correlate with the distribution of PRICKLE2 which remains similar to that seen in wild type animals (Fig. S1). Other factors may therefore override the influence of PCP genes in the *Tecta/b*^{dKO} mice.

The cords of densely-packed filaments that run almost longitudinally along the upper surface of the TM prior to the appearance of collagen fibrils (Fig. 3A) are also slanted towards the apical end of the cochlea, albeit with a far greater offset than that of the collagen fibrils. Their orientation may, nonetheless, depend on PCP within the epithelium. An examination of these cords in control and *PTK7* knockout cochleae failed, however, to reveal any obvious difference in their orientation (Fig. S2).

Discussion

The results of this study can be summarised as follows: (i) a tectorin-based matrix precedes the appearance of collagen fibrils and is required for the formation of co-aligned and near-radially oriented collagen-fibril bundles during the first phase of TM development, (ii) the formation of this highly organised system of collagen fibrils occurs within 24 hours and correlates with a large increase in collagen-fibril numbers, (iii) the near-radial orientation of the collagen fibrils does not appear to be dependent on an increase in the width of the underlying epithelium, (iv) a tectorin-based matrix is not required for the formation of co-

aligned collagen fibrils at later stages of development, (vi) the cilia of the underlying epithelial cells are not required for normal collagen-fibril bundle patterning, (vi) the asymmetric proximo-distal distribution of PRICKLE2 in the underlying epithelial cells correlates with the apically-directed offset of the collagen-fibril bundles in the TM, and (vii) the collagen-fibril bundles of the TM are no longer apically offset in the absence of either *Vangl2* or *Ptk7*.

Using TEM, polymerised collagen fibrils with a diameter of 20 nm are first observed in the TM at E15.5, at least one day after the formation of a thin tectorin-based matrix on the surface of the GER, and 3 days after *Tecta* and *Tectb* mRNA expression begins in this region (Rau et al., 1999). These collagen fibrils lie on and above the microvilli that crown the surfaces of GER cells and below the electron-dense matrix that forms the upper surface of the TM. Immunofluorescence microscopy reveals the collagen at this stage forms fibril bundles that are oriented in an apparently random fashion. By E16.5 these collagen-fibril bundles are longer and co-aligned in a near-radial manner (i.e., replete with an apically-directed offset), a pattern closely resembling that seen in the mature TM. The alignment and orientation of the collagen-fibril bundles therefore happens very rapidly, as the number of collagen fibrils in the TM is increasing, and is therefore likely to be happening in parallel with collagen-fibril polymerisation.

Whilst the apical-basal polarity of the cells in the GER makes it unlikely that fibripositor-like devices are involved in directing collagen orientation in the developing TM, cells located along the inwardly-inclined medial edge of the ridge could pull in polymerised fibrils and extrude them in a radial fashion, much in the same way that fibripositors align collagen fibrils within developing tendons. An extensive search for apical membrane invaginations enveloping collagen fibrils in this region and elsewhere failed, however, to reveal evidence for the existence of such a mechanism. Furthermore, polymerised collagen fibrils were never observed around the basal regions of the microvilli on the GER cells.

It has been known for some time that cells can generate traction forces that can orient extracellular fibres (Harris et al., 1981), and more recent studies have shown that cell colonies grown on a collagenous matrix can induce collagen-fibre alignment (Vader et al., 2009). Inducing strain on Type I collagen gels also results in the post-polymerisation alignment of collagen fibres, providing the induced strain/stretch exceeds 5% (Vader et al., 2009). Cellular growth or cell-based traction have also been implicated in *in vivo* models; fluorescently-labelled collagen injected into developing chick limb buds rearranges and aligns in an injection-site appropriate manner (Stopak et al., 1985). As collagen-fibril alignment and orientation occurs concomitant with a large increase in the apical surface area of a medially-located subset of GER cells, we explored whether an increase in the width of

the epithelium underlying the TM could account for the observed near-radial patterning of collagen fibrils. Our observations, however, suggest otherwise. Alignment and orientation in the basal (IHC10-50) region of the cochlea occurs without an increase in the width of the GER and, in more apical regions, it occurs whilst the length and width of the GER are increasing by a similar amount, suggesting there is unlikely to be a force vector that is greater in the radial dimension.

Nonetheless the alignment and orientation of collagen fibrils within the TM does occur whilst the luminal surface area of the cells in the medial GER is increasing considerably (see Fig. 4C, F), and a previous study of cellular changes in the developing cochlea (McKenzie et al., 2004) has shown that sensory cells immediately lateral to the GER undergo radial intercalation (McKenzie et al., 2004) coupled with an increase in apical surface area, leading to a reduction in the number of cells across the medio-lateral axis of the developing organ of Corti as it undergoes convergent extension. Whilst there is a considerable reduction in the number of cells per unit area in the GER between E15.5 and E16.5 (from 500 to 300 per 5000 um^2, see Fig. S3), which is accompanied by an increase in the surface area of some of the cells (notably those in the medial GER), in the absence of distinct cell types (such as the inner hair cells within the organ of Corti) it is not possible to determine whether radial intercalation is occurring in this region.

Recent evidence has shown that molecular crowding and confinement within a narrow space can have a dramatic effect on the ability of collagen fibrils to align *in vitro* (Saeidi et al., 2012). When concentrated solutions of acid-soluble Type I collagen are neutralised and allowed to polymerise between two glass coverslips, layers of highly-organised, co-aligned collagen fibrils are formed that resemble the lamellae seen, for example, in either the cornea or the anulus fibrosus, leading to the view that physical factors alone may control collagen fibrillogenesis (Saeidi et al., 2012). The upper, dense layer of the developing TM may confine collagen polymerisation to a narrow layer just above the epithelium and, in the *Tecta/b*^{dKO} mouse in which this upper layer is absent, the first collagen-fibril bundles are, indeed, malformed and highly disorganised. Whilst this observation strongly implies confinement plays a role, fibril bundles that form subsequently in the *Tecta/b*^{dKO} mouse are of normal dimension, co-aligned with one another and, at least throughout the apical two thirds of the cochlea, oriented radially across with TM with the expected apical slant/offset. Whilst additional factors (e.g., hyaluronate) may be secreted during the later phase that could cause molecular crowding, it is also possible that the network of disorganised collagen-fibril bundles that initially forms in the *Tecta/b*^{dKO} mouse confines the collagen that forms subsequently, and this is sufficient to enable collagen-fibril bundle co-alignment.

Although an overlying meshwork of disorganised collagen fibrils may substitute for the lack of a tectorin-based matrix during the later stages of TM development in the *Tecta/b*^{dKO} mouse, the later-forming collagen-fibril bundles in the basal third of the cochlea that lie closest to the epithelium are, whilst being co-aligned, incorrectly oriented. At the extreme basal end of the cochlea these lower-layer collagen fibrils run exclusively along the length of the organ of Corti, instead of near-radially, and their orientation does not correlate with the distribution of PRICKLE2. The cochlea continues to grow in length after the early phase of collagen-fibril bundle formation and, if this elongation is largely restricted to the basal part of the cochlea, the forces produced may be sufficient to cause the mis-orientation of the lower-layer collagen-fibril bundles seen in the *Tecta/b*^{dKO} mouse. The tectorin-based matrix could therefore serve an additional function; it may lock the collagen-fibril bundles into place once they have been produced and thereby reduce the impact of external forces.

Although confinement may drive the production of co-aligned collagen-fibril bundles within the developing TM, it cannot alone explain why the co-aligned fibril bundles are near-radially oriented. The active movement of small cilia on cells distributed throughout the otic vesicle of the zebrafish is thought to generate fluid flow important for the normal formation of otoliths (Riley et al., 1997; Yu et al., 2011) and an *in vitro* study of collagen-fibre alignment in microfluidic channels (Lee et al., 2006) has shown confinement of Type I collagen coupled with exposure to a few seconds of fluid flow can generate collagen fibrils that align in parallel (±15°) with the long axis of the chamber. Whilst the cilia of the GER cells have a 9+0 or 9v distribution (Gluenz et al., 2010) of microtubule doublets (RG & GR unpublished) and therefore likely to be non-motile primary cilia, collagen fibrils in the developing TM are associated with these cilia and their movement within the apical pole of the GER cells may direct collagen patterning. However, in the *Kif3a*^{cKO} mouse (Sipe and Lu, 2011), despite a complete absence of cilia and defects in cochlear elongation, the collagen fibrils are still remarkably well co-aligned, with a typical near-radial orientation. The cilia therefore do not play a direct role in this process.

Although cilia of the cells in the GER are not required for the normal orientation of the collagen-fibril bundles in the developing TM, the distribution of PRICKLE2 in the region of the GER underlying the middle of the TM and the loss of an apical offset seen in the conditional *Ptk7* and *Vangl2* mutants clearly indicates that signals from the epithelial cells of the GER can influence collagen patterning in the overlying extracellular matrix. Although mutations in many of the PCP genes lead to convergent extension defects and a shortening of the cochlear duct, and whilst the *PTK7*^{cKO} mouse has a shortened cochlea, the length of the cochlea is normal in the *Vangl2*^{cKO} mice so it is unlikely that an extension defect underlies the observed lack of an apical offset. Furthermore, a distinct radially directed apical

slant in the collagen fibrils is observed in the *Kif3a*^{cKO} mouse in which the cochlea is considerably truncated. The question therefore arises as to how PTK7 and VANGL2 are able to determine the distinctive offset in the radial orientation of the collagen-fibrils bundles in the TM. Evidence from studies of how hair-cell polarity in the organ of Corti is controlled have suggested that PTK7, acting via Src and ROCK, acts in concert with the core PCP pathway (via PRICKLE and JNK) to regulate actomyosin contractility at the cell-cell junctions (Lee et al., 2012; Andreeva et al., 2014). Assuming the default state for collagen-fibril bundle alignment generated by physicochemical forces is strictly radial (Fig. 13A), the PTK7 and VANGL2 dependent asymmetric distribution of PRICKLE2 may result in an actomyosin driven rotation of the terminal web that causes the collagen fibrils lying atop of the microvillar bed to rotate in one direction, with the fibrils that form subsequently templating on those that are deflected during this rotation (Fig. 13B). Alternatively, a constant asymmetrically directed force towards the junctions at the distal edges of the GER cells may be sufficient to generate an apical slant in the collagen fibrils as they are produced (Fig. 13C). In both these models it is assumed the forces are transmitted to the collagen fibrils via the microvilli.

Whilst previous studies have shown that PCP pathway genes can regulate the distribution and assembly of fibronectin during gastrulation (Goto et al., 2005; Dzamba et al., 2009; Dohn et al., 2013) or tissue remodelling (Williams et al., 2012), the results of this study provide, to the best of our knowledge, the first evidence that PCP can fine tune the orientation of collagen-fibril bundles within an extracellular matrix.

Acknowledgements: Supported by The Wellcome Trust (Grant 087377, GR) and National Institutes of Health grants R01DC013773 (XL) and R01DC013066 (MD). The authors would like to thank for Professor Andy Forge at the UCL Ear Institute for his assistance with scanning electron microscopy.

References

Andreeva, A., Lee, J., Lohia, M., Wu, X., Macara, I. G. and Lu, X. (2014). PTK7-Src signaling at epithelial cell contacts mediates spatial organization of actomyosin and planar cell polarity. *Dev. Cell* **29**, 20–33.

Ashmore, J. (2008). Cochlear outer hair cell motility. *Physiol. Rev.* **88**, 173–210.

Canty, E. G., Lu, Y., Meadows, R. S., Shaw, M. K., Holmes, D. F. and Kadler, K. E. (2004). Coalignment of plasma membrane channels and protrusions (fibripositors) specifies the parallelism of tendon. *J. Cell Biol.* **165**, 553–563.

Cohen-Salmon, M., El-Amraoui, A., Leibovici, M. and Petit, C. (1997). Otogelin: a glycoprotein specific to the acellular membranes of the inner ear. *Proc. Natl. Acad. Sci. U.S.A.* **94**, 14450–14455.

Copley, C. O., Duncan, J. S., Liu, C., Cheng, H. and Deans, M. R. (2013). Postnatal refinement of auditory hair cell planar polarity deficits occurs in the absence of Vangl2. *J. Neurosci.* **33**, 14001–14016.

Dallos, P. (2008). Cochlear amplification, outer hair cells and prestin. *Curr. Opin. Neurobiol.* **18**, 370–376.

Davis, H. (1965). A model for transducer action in the cochlea. *Cold Spring Harb. Symp. Quant. Biol.* **30**, 181–190.

Deans, M. R., Antic, D., Suyama, K., Scott, M. P., Axelrod, J. D. and Goodrich, L. V. (2007). Asymmetric distribution of prickle-like 2 reveals an early underlying polarization of vestibular sensory epithelia in the inner ear. *J. Neurosci.* **27**, 3139–3147.

Dohn, M. R., Mundell, N. A., Sawyer, L. M., Dunlap, J. A. and Jessen, J. R. (2013). Planar cell polarity proteins differentially regulate extracellular matrix organization and assembly during zebrafish gastrulation. *Dev. Biol.* **383**, 39–51.

Duance, V. C., Shimokomaki, M. and Bailey, A. J. (1982). Immunofluorescence localization of type-M collagen in articular cartilage. *Biosci. Rep.* **2**, 223–227.

Dzamba, B. J., Jakab, K. R., Marsden, M., Schwartz, M. A. and DeSimone, D. W. (2009). Cadherin adhesion, tissue tension, and noncanonical Wnt signaling regulate fibronectin matrix organization. *Dev. Cell* **16**, 421–432.

Ezan, J. and Montcouquiol, M. (2013). Revisiting planar cell polarity in the inner ear. *Semin. Cell Dev. Biol.* **24**, 499–506.

Gavara, N. and Chadwick, R. S. (2009). Collagen-based mechanical anisotropy of the tectorial membrane: implications for inter-row coupling of outer hair cell bundles. *PLoS ONE* **4**, e4877.

Ghaffari, R., Aranyosi, A. J., Richardson, G. P. and Freeman, D. M. (2010). Tectorial membrane travelling waves underlie abnormal hearing in Tectb mutant mice. *Nat Commun* **1**, 96.

Gluenz, E., Höög, J. L., Smith, A. E., Dawe, H. R., Shaw, M. K. and Gull, K. (2010). Beyond 9+0: noncanonical axoneme structures characterize sensory cilia from protists to humans. *FASEB J.* **24**, 3117–3121.

Goto, T., Davidson, L., Asashima, M. and Keller, R. (2005). Planar cell polarity genes regulate polarized extracellular matrix deposition during frog gastrulation. *Curr. Biol.* **15**, 787–793.

Gummer, A. W., Hemmert, W. and Zenner, H. P. (1996). Resonant tectorial membrane motion in the inner ear: its crucial role in frequency tuning. *Proc Natl Acad Sci U S A* **93**, 8727–8732.

Harris, A. K., Stopak, D. and Wild, P. (1981). Fibroblast traction as a mechanism for collagen morphogenesis. *Nature* **290**, 249–251.

Hasko, J. A. and Richardson, G. P. (1988). The ultrastructural organization and properties of the mouse tectorial membrane matrix. *Hear. Res.* **35**, 21–38.

Kalson, N. S., Starborg, T., Lu, Y., Mironov, A., Humphries, S. M., Holmes, D. F. and Kadler, K. E. (2013). Nonmuscle myosin II powered transport of newly formed collagen fibrils at the plasma membrane. *Proc. Natl. Acad. Sci. U.S.A.* **110**, E4743-4752.

Kammerer, R., Rüttiger, L., Riesenberg, R., Schäuble, C., Krupar, R., Kamp, A., Sunami, K., Eisenried, A., Hennenberg, M., Grunert, F., et al. (2012). Loss of mammal-specific tectorial membrane component carcinoembryonic antigen cell adhesion molecule 16 (CEACAM16) leads to hearing impairment at low and high frequencies. *J. Biol. Chem.* **287**, 21584–21598.

Kapacee, Z., Richardson, S. H., Lu, Y., Starborg, T., Holmes, D. F., Baar, K. and Kadler, K. E. (2008). Tension is required for fibripositor formation. *Matrix Biol.* **27**, 371–375.

Kelley, M. W. (2007). Cellular commitment and differentiation in the organ of Corti. *Int. J. Dev. Biol.* **51**, 571–583.

Knipper, M., Richardson, G., Mack, A., Müller, M., Goodyear, R., Limberger, A., Rohbock, K., Köpschall, I., Zenner, H. P. and Zimmermann, U. (2001). Thyroid hormone-deficient period prior to the onset of hearing is associated with reduced levels of beta-tectorin protein in the tectorial membrane: implication for hearing loss. *J. Biol. Chem.* **276**, 39046–39052.

Lee, P., Lin, R., Moon, J. and Lee, L. P. (2006). Microfluidic alignment of collagen fibers for in vitro cell culture. *Biomed Microdevices* **8**, 35–41.

Lee, J., Andreeva, A., Sipe, C. W., Liu, L., Cheng, A. and Lu, X. (2012). PTK7 regulates myosin II activity to orient planar polarity in the mammalian auditory epithelium. *Curr. Biol.* **22**, 956–966.

Legan, P. K., Rau, A., Keen, J. N. and Richardson, G. P. (1997). The mouse tectorins. Modular matrix proteins of the inner ear homologous to components of the sperm-egg adhesion system. *J. Biol. Chem.* **272**, 8791–8801.

Legan, P. K., Lukashkina, V. A., Goodyear, R. J., Kössi, M., Russell, I. J. and Richardson, G. P. (2000). A targeted deletion in alpha-tectorin reveals that the tectorial membrane is required for the gain and timing of cochlear feedback. *Neuron* **28**, 273–285.

Legan, P. K., Lukashkina, V. A., Goodyear, R. J., Lukashkin, A. N., Verhoeven, K., Van Camp, G., Russell, I. J. and Richardson, G. P. (2005). A deafness mutation isolates a second role for the tectorial membrane in hearing. *Nat. Neurosci.* **8**, 1035–1042.

Lim, D. J. (1972). Fine morphology of the tectorial membrane. Its relationship to the organ of Corti. *Arch Otolaryngol* **96**, 199–215.

Lim, D. J. (1987). Development of the tectorial membrane. *Hear. Res.* **28**, 9–21.

Lu, X. and Sipe, C. W. (2016). Developmental regulation of planar cell polarity and hair-bundle morphogenesis in auditory hair cells: lessons from human and mouse genetics. *Wiley Interdiscip Rev Dev Biol* **5**, 85–101.

Lukashkin, A. N., Richardson, G. P. and Russell, I. J. (2010). Multiple roles for the tectorial membrane in the active cochlea. *Hear. Res.* **266**, 26–35.

May-Simera, H. and Kelley, M. W. (2012). Planar cell polarity in the inner ear. *Curr. Top. Dev. Biol.* **101**, 111–140.

McKenzie, E., Krupin, A. and Kelley, M. W. (2004). Cellular growth and rearrangement during the development of the mammalian organ of Corti. *Dev. Dyn.* **229**, 802–812.

Meaud, J. and Grosh, K. (2010). The effect of tectorial membrane and basilar membrane longitudinal coupling in cochlear mechanics. *J. Acoust. Soc. Am.* **127**, 1411–1421.

Montcouquiol, M., Rachel, R. A., Lanford, P. J., Copeland, N. G., Jenkins, N. A. and Kelley, M. W. (2003). Identification of Vangl2 and Scrb1 as planar polarity genes in mammals. *Nature* **423**, 173–177.

Nowotny, M. and Gummer, A. W. (2006). Nanomechanics of the subtectorial space caused by electromechanics of cochlear outer hair cells. *Proc. Natl. Acad. Sci. U.S.A.* **103**, 2120–2125.

Rau, A., Legan, P. K. and Richardson, G. P. (1999). Tectorin mRNA expression is spatially and temporally restricted during mouse inner ear development. *J. Comp. Neurol.* **405**, 271–280.

Richardson, G. P., Russell, I. J., Duance, V. C. and Bailey, A. J. (1987). Polypeptide composition of the mammalian tectorial membrane. *Hear. Res.* **25**, 45–60.

Riley, B. B., Zhu, C., Janetopoulos, C. and Aufderheide, K. J. (1997). A critical period of ear development controlled by distinct populations of ciliated cells in the zebrafish. *Dev. Biol.* **191**, 191–201.

Russell, I. J., Legan, P. K., Lukashkina, V. A., Lukashkin, A. N., Goodyear, R. J. and Richardson, G. P. (2007). Sharpened cochlear tuning in a mouse with a genetically modified tectorial membrane. *Nat. Neurosci.* **10**, 215–223.

Saeidi, N., Karmelek, K. P., Paten, J. A., Zareian, R., DiMasi, E. and Ruberti, J. W. (2012). Molecular crowding of collagen: a pathway to produce highly-organized collagenous structures. *Biomaterials* **33**, 7366–7374.

Sipe, C. W. and Lu, X. (2011). Kif3a regulates planar polarization of auditory hair cells through both ciliary and non-ciliary mechanisms. *Development* **138**, 3441–3449.

Stopak, D., Wessells, N. K. and Harris, A. K. (1985). Morphogenetic rearrangement of injected collagen in developing chicken limb buds. *Proc. Natl. Acad. Sci. U.S.A.* **82**, 2804–2808.

Thalmann, I. (1993). Collagen of accessory structures of organ of Corti. *Connect. Tissue Res.* **29**, 191–201.

Vader, D., Kabla, A., Weitz, D. and Mahadevan, L. (2009). Strain-induced alignment in collagen gels. *PLoS ONE* **4**, e5902.

Wang, J., Mark, S., Zhang, X., Qian, D., Yoo, S.-J., Radde-Gallwitz, K., Zhang, Y., Lin, X., Collazo, A., Wynshaw-Boris, A., et al. (2005). Regulation of polarized extension and planar cell polarity in the cochlea by the vertebrate PCP pathway. *Nat. Genet.* **37**, 980–985.

Wang, Y., Guo, N. and Nathans, J. (2006). The role of Frizzled3 and Frizzled6 in neural tube closure and in the planar polarity of inner-ear sensory hair cells. *J. Neurosci.* **26**, 2147–2156.

Williams, B. B., Mundell, N., Dunlap, J. and Jessen, J. (2012). The planar cell polarity protein VANGL2 coordinates remodeling of the extracellular matrix. *Commun Integr Biol* **5**, 325–328.

Yariz, K. O., Duman, D., Zazo Seco, C., Dallman, J., Huang, M., Peters, T. A., Sirmaci, A., Lu, N., Schraders, M., Skromne, I., et al. (2012). Mutations in OTOGL, encoding the inner ear protein otogelin-like, cause moderate sensorineural hearing loss. *Am. J. Hum. Genet.* **91**, 872–882.

Yu, X., Lau, D., Ng, C. P. and Roy, S. (2011). Cilia-driven fluid flow as an epigenetic cue for otolith biomineralization on sensory hair cells of the inner ear. *Development* **138**, 487–494.

Zheng, J., Miller, K. K., Yang, T., Hildebrand, M. S., Shearer, A. E., DeLuca, A. P., Scheetz, T. E., Drummond, J., Scherer, S. E., Legan, P. K., et al. (2011). Carcinoembryonic antigen-related cell adhesion molecule 16 interacts with alpha-tectorin and is mutated in autosomal dominant hearing loss (DFNA4). *Proc. Natl. Acad. Sci. U.S.A.* **108**, 4218–4223.

Figure legends

Figure1. **Organ of Corti and tectorial membrane structure.** A) Schematic drawing of the mature mouse organ of Corti. The TM (blue) attaches to the spiral limbus and the tips of

OHC hair bundles. Specialised peripheral features include covernet fibrils, marginal band and Hensen's stripe. Collagen fibrils run across the TM. B) Surface view of a mature Alcian-blue stained TM (DIC optics). The covernet fibrils and marginal band run along the TM whilst the collagen-fibril bundles are aligned near-radially, with a slight apically-directed (small arrows) slant. C) Drawings showing the organisation of collagen-fibril bundles with respect to the hair bundles of the inner and outer hair cells. Collagen fibrils are oriented with a (15-25^{o}) bias towards the apex. IHCs, inner hair cells; OHCs, outer hair cells. Bar in B = 10 μm.

Figure 2. **Matrix molecule distribution in the developing tectorial membrane.** TECTA (A, E, I), TECTB (B, F, J), OTOGELIN (C, G, K) and COL9A (D, H, L) distribution (green) in the mouse cochlea at E14.5 (A-D), E15.5 (E-H) and E16.5 (I-L). Sections are counterstained for F-ACTIN (magenta). TECTA and TECTB are readily observed at E14.5 (A, B). OTOG staining of the TM is weak at E14.5 (arrow in C). COL9A is not detected in the TM until E15.5 (arrow in H). By E16.5, TECTA staining is seen throughout the TM (I), whereas TECTB and OTOG are concentrated within the upper region (arrowheads in J and K). GER, greater epithelial ridge; HCs, hair cells. Bar = 50 μm.

Figure 3. **Ultrastructure of the developing tectorial membrane.** A) Scanning electron micrograph showing the surface of the TM in the basal cochlea at E14.5. Matrix in the upper layer is organised as thick fibrils that run longitudinally (double arrowheads). B-D) TEM images from radial sections of the TM in the basal cochlea at E14.5 (B), E15.5 (C) and E16.5 (D). B) Double arrowheads indicate dense, upper-layer fibrils shown in A above. Single arrowheads point to the lower layer of loosely-packed fibrillar material. C) Arrows indicate randomly-orientated collagen-fibril bundles first observed at E15.5. D) Arrows in D indicate the radially-oriented collagen fibril-bundles seen by E16.5. Bar in A = 5 μm, Bar in D = 1 μm and applies to B-D.

Figure 4. **Collagen-fibril orientation in the developing tectorial membrane.** Confocal z-projections from equivalent regions of the cochlea, ~130 inner hair cells (IHCs) away from the basal end, from E15.5 (A-C) and E16.5 (D-F) embryos double-stained with phalloidin (magenta in A, D) anti-COL9A (green in A, D). Single-channel images of COL9A (B, E) and phalloidin staining (C, F) are also shown. Tangled, disorganised collagen fibril-bundles are seen at E15.5 (A, B), At E16.5 collagen fibril-bundles form a highly-organised, near-radially oriented array (D, E). Apical cell-surface size increases between E15.5 (C) and E16.5 (F) within the medial GER. Bar = 20 μm.

Figure 5. **Quantification of epithelial dimensions.** A) Photomontage of confocal z-projections from the basal region of a heterozygous *Tecta/b*^{dKO} cochlea at E17.5 stained to amplify EGFP (green) and highlight F-ACTIN (magenta). Numbers indicate cumulative IHC-count from the basal end, asterisk indicates region used for projections shown in B-D. B-D) Orthogonal projections from the 70 IHC region of heterozygous *Tecta/b*^{dKO} mice double-labelled for GFP (green) and TECTA (magenta). Arrows demarcate GER regions from which measurements were taken. E) Graph showing the change in width of the GER region between E15.5, E16.5 and E17.5. Measurements were made at points 10-110 IHCs from basal end of the cochlea. Values at E16.5 and E17.5 significantly different (two-way ANOVA with Dunnett's multiple comparison tests comparing E15.5 with E16.5, and E16.5 with E17.5 at each IHC point) from those at E15.5 and E16.5, respectively, are indicated by asterisks (* $P<0.05$, ** $P<0.01$, **** $P<0.0001$), n=6 (E15.5), n=5 (E16.5 and E 17.5), ns denotes not significant ($P\geq0.05$). F) Relative length of the 10-110 IHC region at E15.5, E16.5 and E17.5. Lengths of entire cochleae are shown to the right. n numbers ± standard deviations are also shown, n refers to individual cochleae from different animals. Bar in A = 100 μm, bar in D = 50 μm and applies to B-D.

Figure 6. **Collagen-fibril orientation in *Tecta/b*^{dKO} mice.** A-D) Confocal z-projections of the GER in the basal cochlea of wild-type (A, C) and *Tecta/b*^{dKO} (B, D) mice at E15.5 (A, B) and E16.5 (C, D) stained with anti-COL9A (green) and phalloidin (magenta). Collagen-fibril bundles in wild-type mice become co-aligned and near-radially oriented between E15.5 and 16.5, those in the *Tecta/b*^{dKO} mice do not. Collagen-fibril bundles in the mutant (B, D) are randomly organised and thicker than those of the wild type (A, C). E-F) TEM images from transverse sections through the basal cochlea at E16.5 in wild-type (E) and *Tecta/b*^{dKO} (F) mice. The dense upper layer of matrix (arrow in E) in the wild-type mouse is absent in the mutant (F). Arrowheads indicate mis-oriented collagen fibrils in the mutant (F). Bar in D = 20 μm. Bar in F = 1 μm.

Figure 7. **Collagen-fibril orientation in later-stage *Tecta/b*^{dKO} mice.** A) Confocal z-projection from the basal cochlea in a P3 *Tecta/b*^{dKO} mouse stained with anti-COL9A (green) and phalloidin (magenta). B-C) Confocal z-projections (~20 microns depth) of COL9A distribution from upper (B) and lower (C) layers of the TM shown in panel A. Collagen-fibril bundles in the upper layer (B) are thicker and have multiple orientations. Those in lower layer (C) are thinner, co-aligned and oriented near-radially but with a basal offset. D) TEM image from a transverse section through the basal region of a *Tecta/b*^{dKO} cochlea at P3. Note that large mis-oriented collagen-fibril bundles (arrowhead) sit above the radially-aligned

lower-layer collagen-fibril bundles (arrows). Bar in C = 20 μm and applies to A-C. Bars in D = 1 μm.

Figure 8. **Mis-oriented collagen in lower layer of later-stage *Tecta/b*^{dKO} mice.** Comparison of TM collagen-fibril bundle orientation in wild-type (A, C, E) and *Tecta/b*^{dKO} (B, D, F, G) cochleae at P3. COL9A staining is shown in green (A-D) and in single-channel panels (E-F). A-B) Basal-coil z-projections including the entire depth of the TM (A, wild type) or the lower 20 microns (B, *Tecta/b*^{dKO}). Collagen-fibril bundles are aligned with an apical slant in the wild-type cochlea (arrow in A). Co-aligned fibrils of the *Tecta/b*^{dKO} TM in this region slant basally (arrow in B). C) Collagen-fibril bundles in the wild-type cochlea slant apically (right-most two arrows in C), except in the basal-most region where they slant basally (left-most two arrows in C). D) At the basal end of *Tecta/b*^{dKO} cochleae, collagen-fibril bundles are aligned longitudinally (arrows in D). G) Photomontage of TM dissected from a P3 *Tecta/b*^{dKO} mouse. Arrows indicate orientation of aligned collagen-fibril bundles at points along the length. Bar in B = 20 μm and applies to A-B, bar in F = 20 μm and applies to C-F, bar in G = 200 μm.

Figure 9. **Cilial attachments of collagen fibrils.** A) TEM image from the GER of a wild-type cochlea at E17.5. Collagen fibrils are associated with the tips of microvilli and cilia (arrow). B) Scanning electron micrograph of the organ of Corti from a *Tecta/b*^{dKO} cochlea at E17.5. Tips of collagen-fibril bundles are often attached to the cilia of underlying cells (arrows). Bar in A = 500 nm, B = 2 μm.

Figure 10. **Collagen patterning in *Kif3a*^{cKO} mice**. A-F) Acetylated tubulin (A-B, D-E) and phalloidin staining (A, C, D, F) in heterozygous control (A-C) and *Kif3a*^{cKO} (D-F) cochleae at E16.5. Cilia can be seen on the surface of GER cells in control (arrows in A, B) but not *Kif3a*^{cKO} mice. Inserts in B and E are x3 enlargements of the boxed regions from the respective panels. G-H) COL9A staining in a heterozygous control (G) and a *Kif3a*^{cKO} mouse at E18.5. Fibril orientation and alignment are similar in mutant and control mice. All images are from the basal cochlea. Bar in F = 20 μm and applies to A-F, bar in H = 20 μm and applies to G-H.

Figure 11. **PRICKLE2 distribution in underlying epithelium.** PRICKLE2 staining (green) within the GER of a P2 wild-type mouse at regions 40% (A), 75% (B) and 90% (C) from the base of the cochlea. F-ACTIN labelling is also shown. PRICKLE2 is asymmetrically distributed around the apical pole of cells located in a narrow band within the GER,

generating lines of staining that run in a medio-lateral direction with a slant that progressively increases towards the apex of the cochlea (compare orientation of arrows in A, B and C). Bar = 20 μm.

Figure 12. **PRICKLE2 distribution in *Vangl2*^{CKO} and *PTK7*^{CKO} mice.** Equivalent mid-coil regions of P1 cochleae double labelled for PRICKLE2 and F-ACTIN (A-F), or COL9A and F-ACTIN (G-L), from control (A-B, G-H), *Vangl2*^{CKO} (C-D, I-J) and *PTK7*^{CKO} (E-F, K-L) mice. PRICKLE2 staining is asymmetrically distributed within a longitudinal stripe within the GER in control animals (A-B') but not in *Vangl2*^{CKO} (C-D') or *PTK7*^{CKO} (E-F') mutants. B', D' and F' show x3 enlargements of PRICKLE2 staining shown in B, D and F respectively. In wild-type mice collagen-fibril bundles have an apically-directed slant (G-H). In the *Vangl2*^{CKO} (I-J) and *PTK7*^{CKO} (K-L) mutant mice collagen-fibril bundles are oriented in an almost perfectly radial fashion. Bar = 20 μm.

Figure 13. **Proposed models.** Two potential models (B, C) for generating apically-offset collagen-fibril bundles. A) Default state, in which collagen fibrils have a purely radial orientation. B) A one-time, PRICKLE2-dependent, actomyosin-generated rotational force reorients collagen fibrils, with subsequently produced fibrils also having a similar orientation due to templating. C) A constant, actomyosin-generated force towards the distally-localised PRICKLE2 results in collagen fibrils adopting an apical slant as they are produced. Forces are assumed to be transmitted from the junctions to the collagen fibrils via the microvilli on the surfaces of the GER cells.

Figure 1

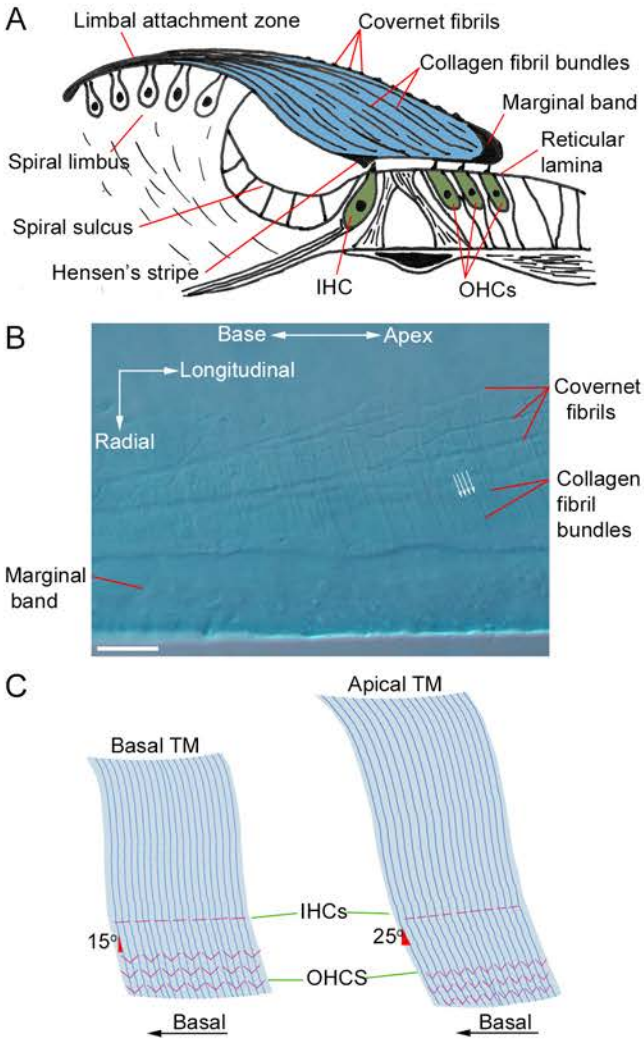

Figure1. **Organ of Corti and tectorial membrane structure**. A) Schematic drawing of the mature mouse organ of Corti. The TM (blue) attaches to the spiral limbus and the tips of OHC hair bundles. Specialised peripheral features include covernet fibrils, marginal band and Hensen's stripe. Collagen fibrils run across the TM. B) Surface view of a mature Alcian-blue stained TM (DIC optics). The covernet fibrils and marginal band run along the TM whilst the collagen-fibril bundles are aligned near-radially, with a slight apically-directed (small arrows) slant. C) Drawings showing the organisation of collagen-fibril bundles with respect to the hair bundles of the inner and outer hair cells. Collagen fibrils are oriented with a (15-25°) bias towards the apex. IHCs, inner hair cells; OHCs, outer hair cells. Bar in B = 10 μm.

Figure 2

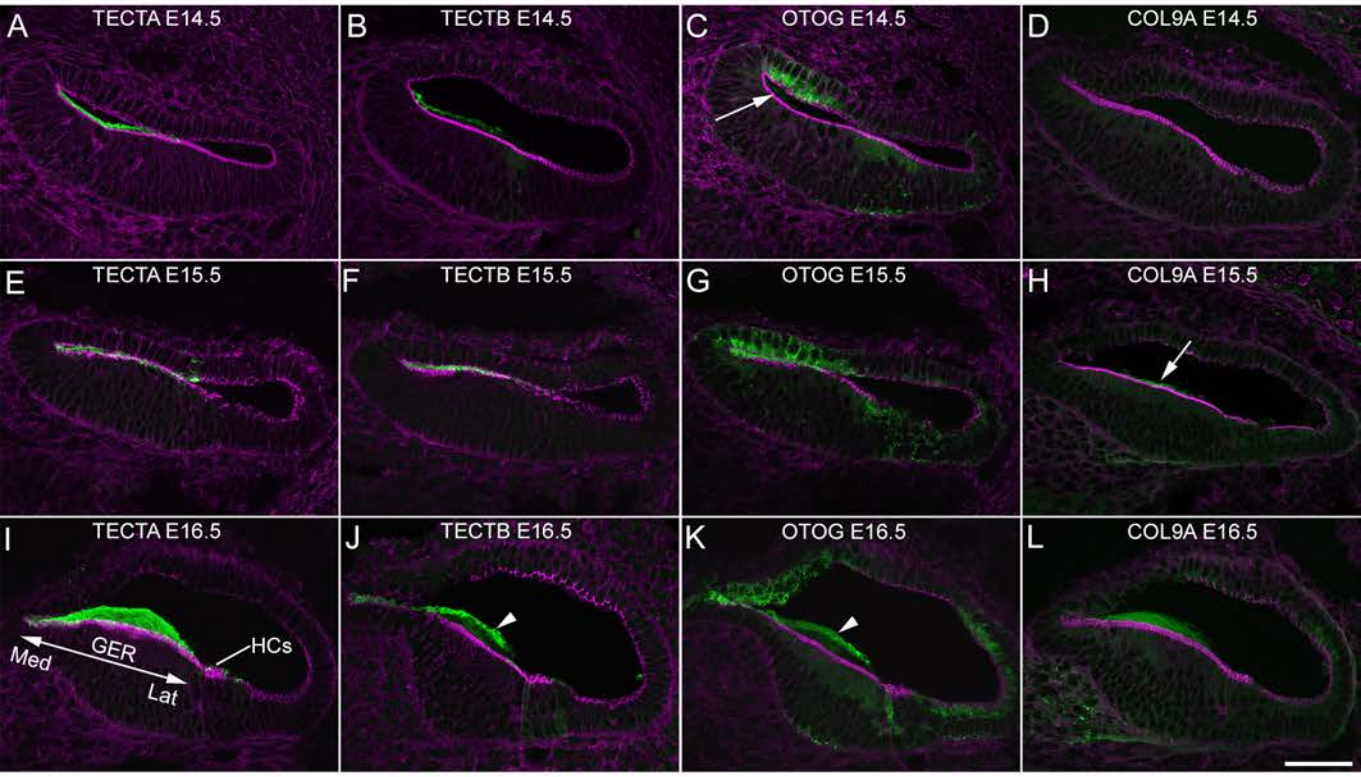

Figure 2. **Matrix molecule distribution in the developing tectorial membrane.** TECTA (A, E, I), TECTB (B, F, J), OTOGELIN (C, G, K) and COL9A (D, H, L) distribution (green) in the mouse cochlea at E14.5 (A-D), E15.5 (E-H) and E16.5 (I-L). Sections are counterstained for F-ACTIN (magenta). TECTA and TECTB are readily observed at E14.5 (A, B). OTOG staining of the TM is weak at E14.5 (arrow in C). COL9A is not detected in the TM until E15.5 (arrow in H). By E16.5, TECTA staining is seen throughout the TM (I), whereas TECTB and OTOG are concentrated within the upper region (arrowheads in J and K). GER, greater epithelial ridge; HCs, hair cells. Bar = 50 μm.

Figure 3

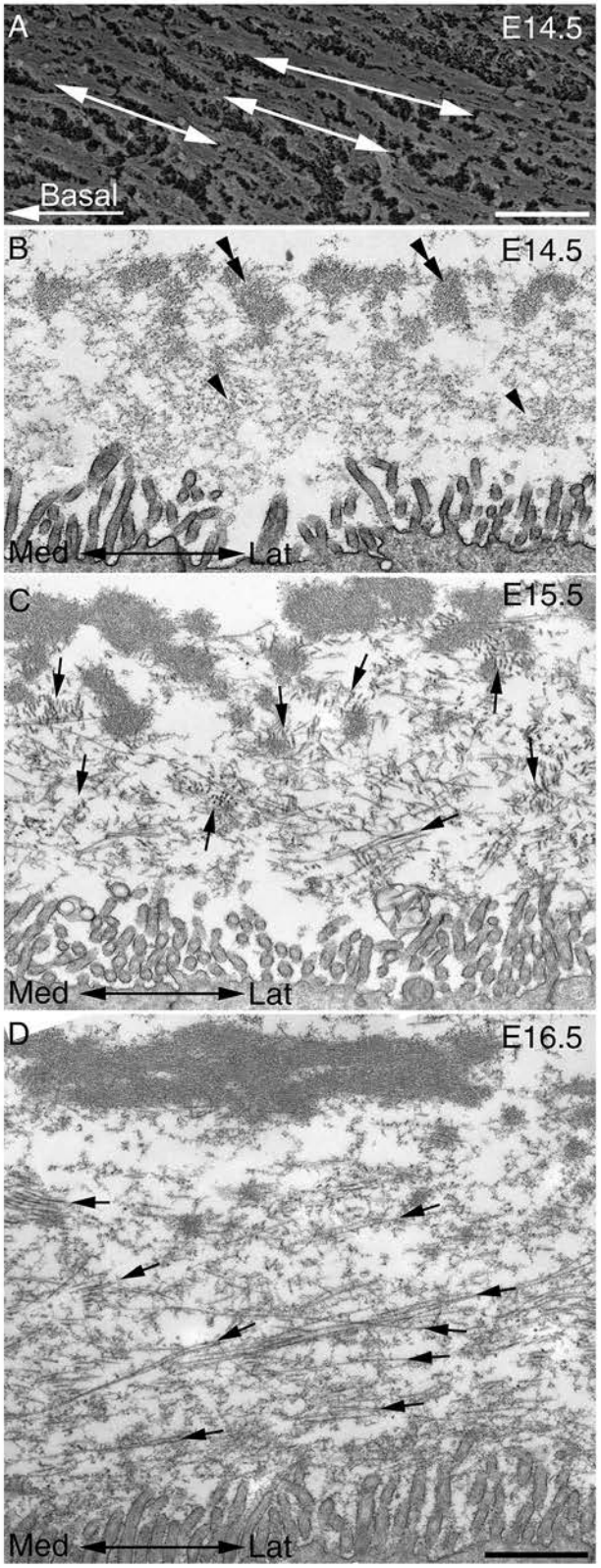

Figure 3. **Ultrastructure of the developing tectorial membrane.** A) Scanning electron micrograph showing the surface of the TM in the basal cochlea at E14.5. Matrix in the upper layer is organised as thick fibrils that run longitudinally (double arrowheads). B-D) TEM images from radial sections of the TM in the basal cochlea at E14.5 (B), E15.5 (C) and E16.5 (D). B) Double arrowheads indicate dense, upper-layer fibrils shown in A above. Single arrowheads point to the lower layer of loosely-packed fibrillar material. C) Arrows indicate randomly-orientated collagen-fibril bundles first observed at E15.5. D) Arrows in D indicate the radially-oriented collagen fibril-bundles seen by E16.5. Bar in A = 5 μm, Bar in D = 1 μm and applies to B-D.

Figure 4

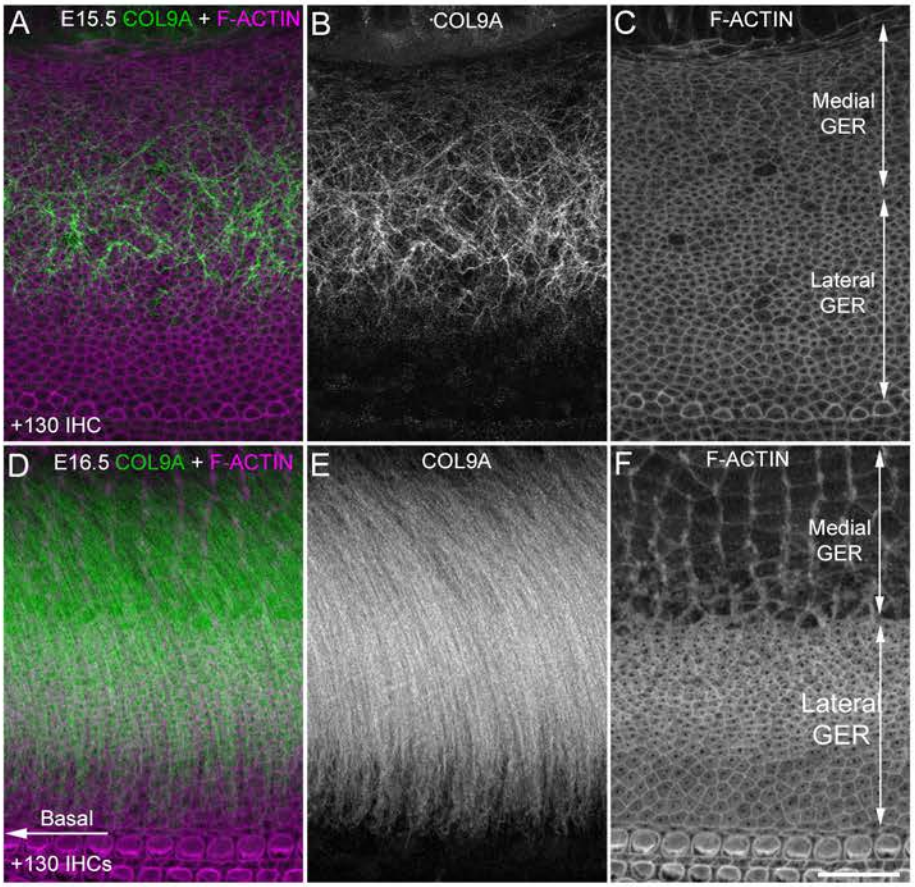

Figure 4. **Collagen-fibril orientation in the developing tectorial membrane.** Confocal z-projections from equivalent regions of the cochlea, ~130 inner hair cells (IHCs) away from the basal end, from E15.5 (A-C) and E16.5 (D-F) embryos double-stained with phalloidin (magenta in A, D) anti-COL9A (green in A, D). Single-channel images of COL9A (B, E) and phalloidin staining (C, F) are also shown. Tangled, disorganised collagen fibril-bundles are seen at E15.5 (A, B), At E16.5 collagen fibril-bundles form a highly-organised, near-radially oriented array (D, E). Apical cell-surface size increases between E15.5 (C) and E16.5 (F) within the medial GER. Bar = 20 μm.

Figure 5

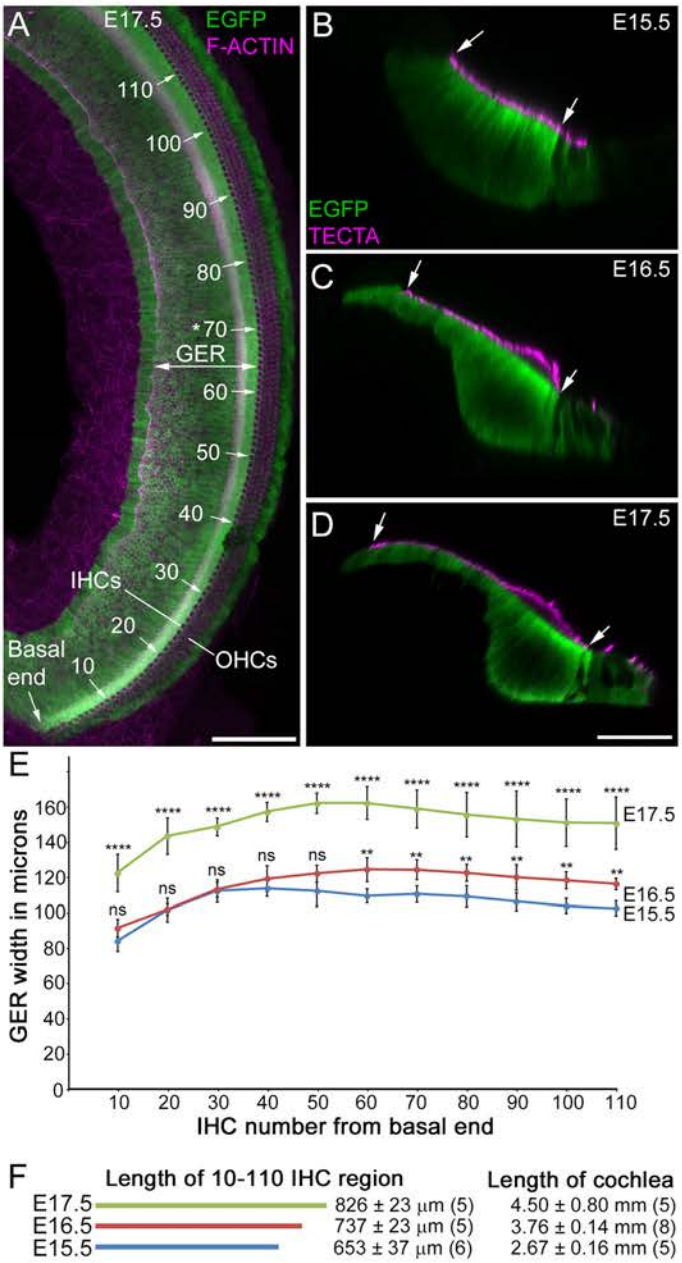

Figure 5. **Quantification of epithelial dimensions**. A) Photomontage of confocal z-projections from the basal region of a heterozygous *Tecta/b*^{dKO} cochlea at E17.5 stained to amplify EGFP (green) and highlight F-ACTIN (magenta). Numbers indicate cumulative IHC-count from the basal end, asterisk indicates region used for projections shown in B-D. B-D) Orthogonal projections from the 70 IHC region of heterozygous *Tecta/b*^{dKO} mice double-labelled for GFP (green) and TECTA (magenta). Arrows demarcate GER regions from which measurements were taken. E) Graph showing the change in width of the GER region between E15.5, E16.5 and E17.5. Measurements were made at points 10-110 IHCs from basal end of the cochlea. Values at E16.5 and E17.5 significantly different (two-way ANOVA with Dunnett's multiple comparison tests comparing E15.5 with E16.5, and E16.5 with E17.5 at each IHC point) from those at E15.5 and E16.5, respectively, are indicated by asterisks (* P<0.05, ** P<0.01, **** P<0.0001, n=6 (E15.5), n=5 (E16.5 and E 17.5), ns denotes not significant (P≥0.05). F) Relative length of the 10-110 IHC region at E15.5, E16.5 and E17.5. Lengths of entire cochleae are shown to the right. n numbers ± standard deviations are also shown, n refers to individual cochleae from different animals. Bar in A = 100 μm, bar in D = 50 μm and applies to B-D.

Figure 6

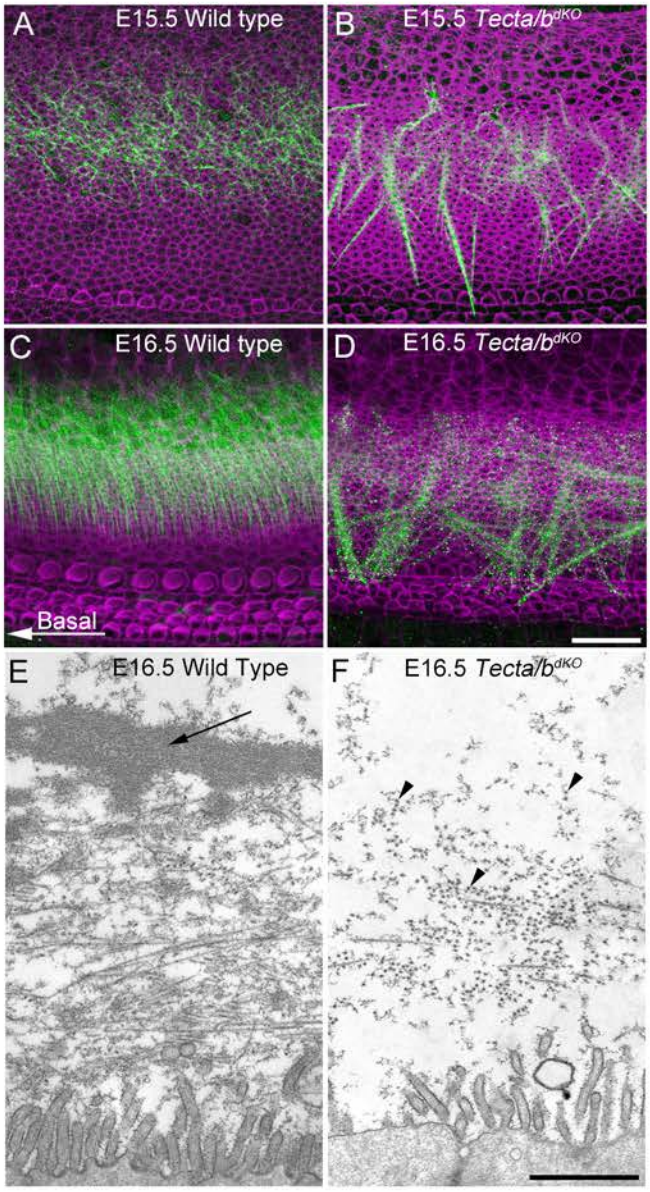

Figure 6. **Collagen-fibril orientation in *Tecta/b^{dKO}* mice**. A-D) Confocal z-projections of the GER in the basal cochlea of wild-type (A, C) and *Tecta/b^{dKO}* (B, D) mice at E15.5 (A, B) and E16.5 (C, D) stained with anti-COL9A (green) and phalloidin (magenta). Collagen-fibril bundles in wild-type mice become co-aligned and near-radially oriented between E15.5 and 16.5, those in the *Tecta/b^{dKO}* mice do not. Collagen-fibril bundles in the mutant (B, D) are randomly organised and thicker than those of the wild type (A, C). E-F) TEM images from transverse sections through the basal cochlea at E16.5 in wild-type (E) and *Tecta/b^{dKO}* (F) mice. The dense upper layer of matrix (arrow in E) in the wild-type mouse is absent in the mutant (F). Arrowheads indicate mis-oriented collagen fibrils in the mutant (F). Bar = 20 μm.

Figure 7

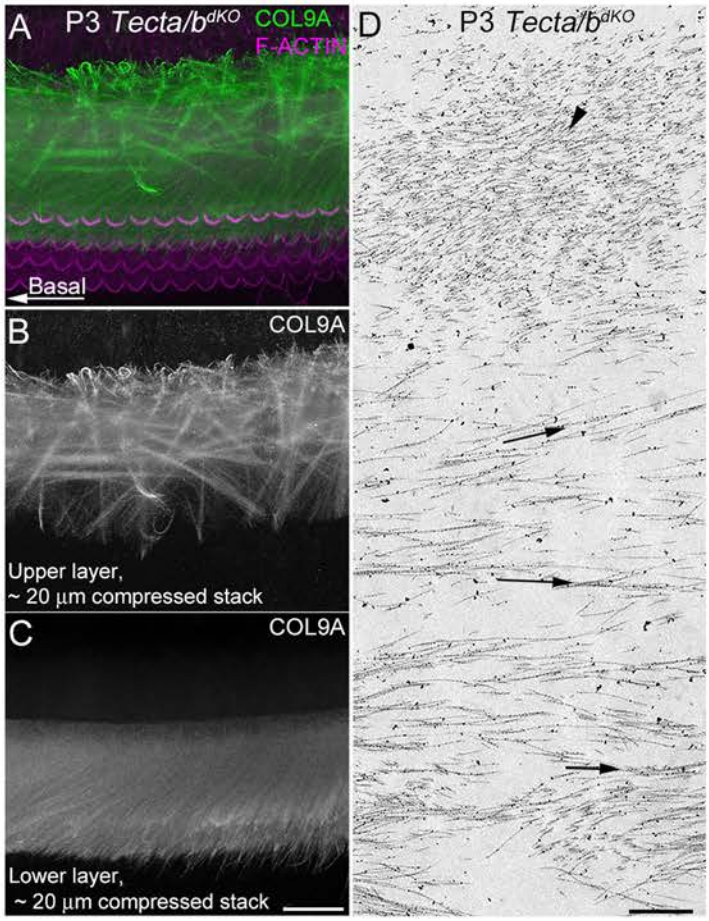

Figure 7. **Collagen-fibril orientation in later-stage *Tecta/b*^{dKO} mice**. A) Confocal z-projection from the basal cochlea in a P3 *Tecta/b*^{dKO} mouse stained with anti-COL9A (green) and phalloidin (magenta). B-C) Confocal z-projections (~20 microns depth) of COL9A distribution from upper (B) and lower (C) layers of the TM shown in panel A. Collagen-fibril bundles in the upper layer (B) are thicker and have multiple orientations. Those in lower layer (C) are thinner, co-aligned and oriented near-radially but with a basal offset. D) TEM image from a transverse section through the basal region of a *Tecta/b*^{dKO} cochlea at P3. Note that large mis-oriented collagen-fibril bundles (arrowhead) sit above the radially-aligned lower-layer collagen-fibril bundles (arrows). Bar in C = 20 μm and applies to A-C. Bars in D = 1 μm.

Figure 8

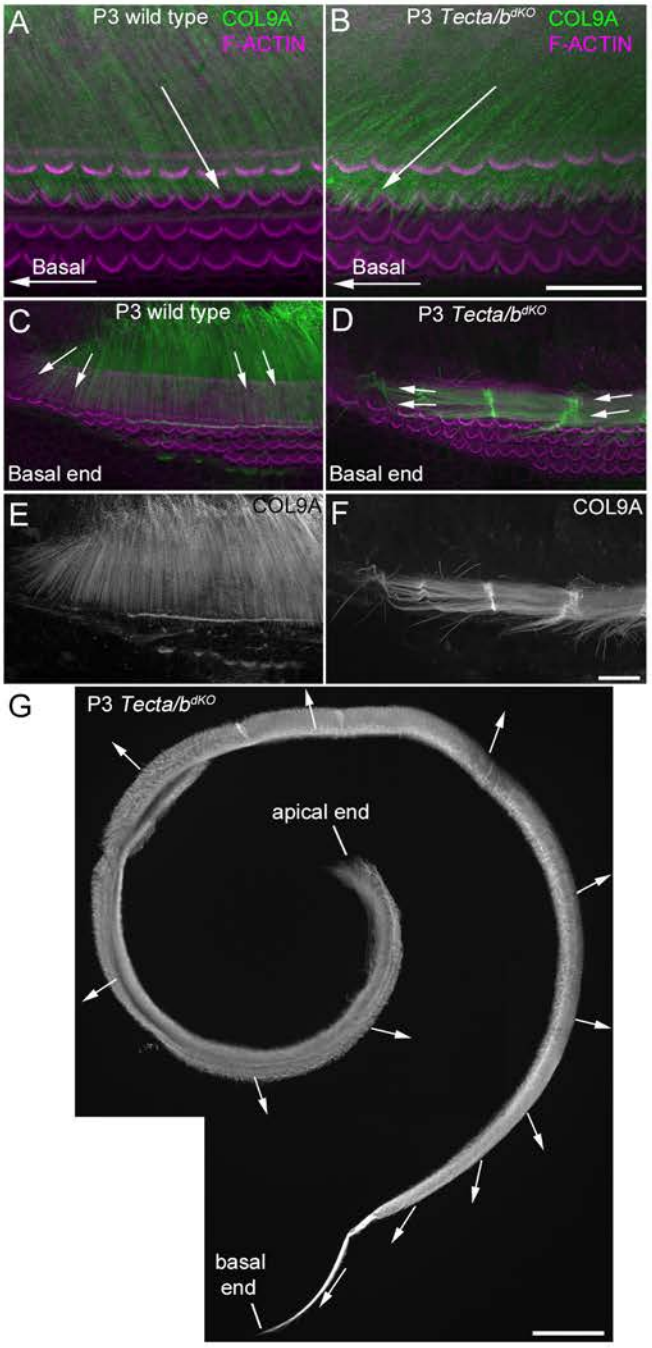

Figure 8. **Mis-oriented collagen in lower layer of later-stage *Tecta/b*^{dKO} mice**. Comparison of TM collagen-fibril bundle orientation in wild-type (A, C, E) and *Tecta/b*^{dKO} (B, D, F, G) cochleae at P3. COL9A staining is shown in green (A-D) and in single-channel panels (E-F). A-B) Basal-coil z-projections including the entire depth of the TM (A, wild type) or the lower 20 microns (B, *Tecta/b*^{dKO}). Collagen-fibril bundles are aligned with an apical slant in the wild-type cochlea (arrow in A). Co-aligned fibrils of the *Tecta/b*^{dKO} TM in this region slant basally (arrow in B). C) Collagen-fibril bundles in the wild-type cochlea slant apically (right-most two arrows in C), except in the basal-most region where they slant basally (left-most two arrows in C). D) At the basal end of *Tecta/b*^{dKO} cochleae, collagen-fibril bundles are aligned longitudinally (arrows in D). G) Photomontage of TM dissected from a P3 *Tecta/b*^{dKO} mouse. Arrows indicate orientation of aligned collagen-fibril bundles at points along the length. Bar in B = 20 μm and applies to A-B, bar in F = 20 μm and applies to C-F, bar in G = 200 μm.

Figure 9

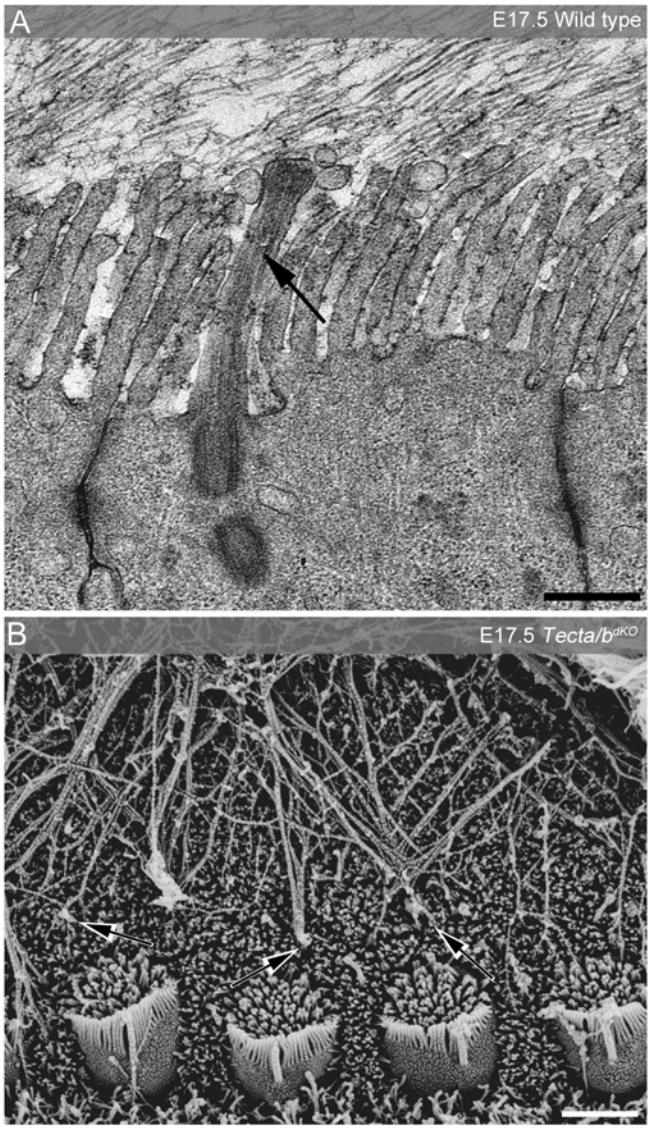

Figure 9. **Cilial attachments of collagen fibrils.** A) TEM image from the GER of a wild-type cochlea at E17.5. Collagen fibrils are associated with the tips of microvilli and cilia (arrow). B) Scanning electron micrograph of the organ of Corti from a *Tecta/b*^{dKO} cochlea at E17.5. Tips of collagen-fibril bundles are often attached to the cilia of underlying cells (red arrows). Bar in A = 500 nm, B = 2 μm.

Figure 10

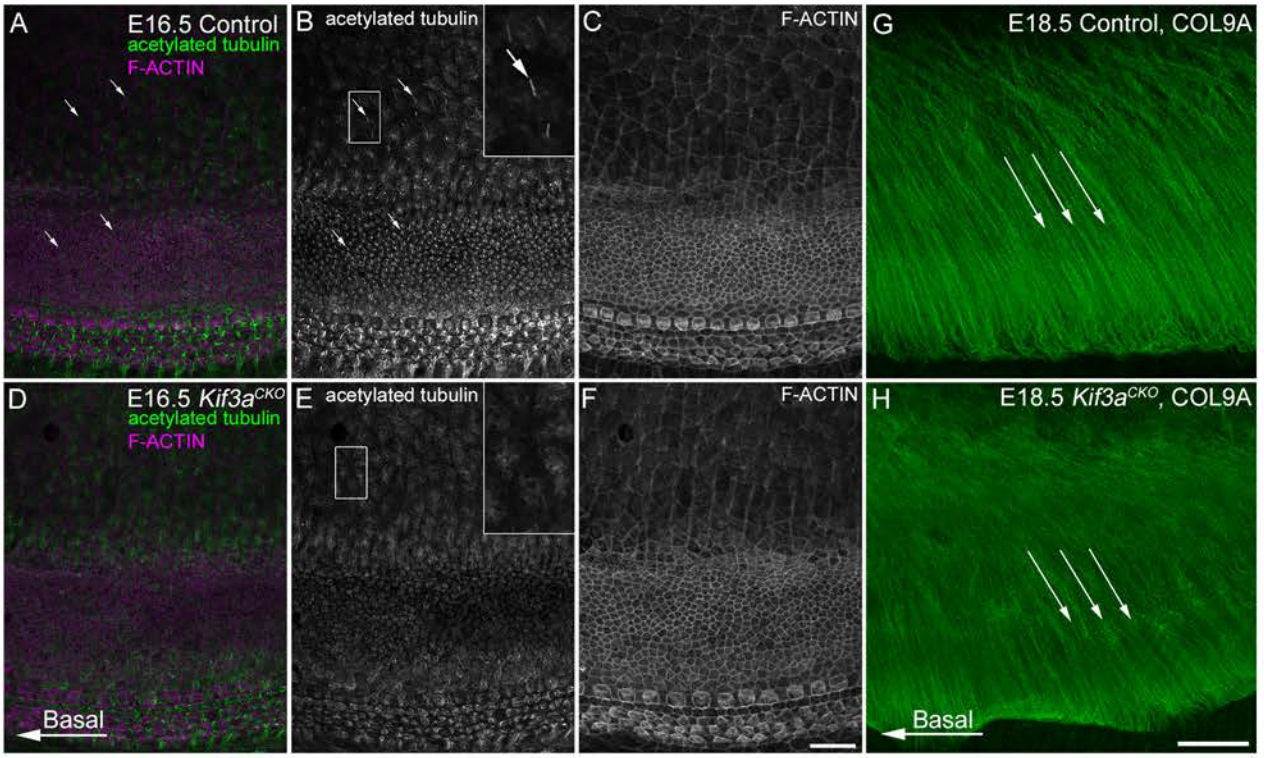

Figure 10. **Collagen patterning in *Kif3a*^{cKO} mice.** A-F) Acetylated tubulin (A-B, D-E) and phalloidin staining (A, C, D, F) in heterozygous control (A-C) and *Kif3a*^{cKO} (D-F) cochleae at E16.5. Cilia can be seen on the surface of GER cells in control (arrows in A, B) but not *Kif3a*^{cKO} mice. Inserts in B and E are x3 enlargements of the boxed regions from the respective panels. G-H) COL9A staining in a heterozygous control (G) and a *Kif3a*^{cKO} mouse at E18.5. Fibril orientation and alignment are similar in mutant and control mice. All images are from the basal cochlea. Bar in F = 20 μm and applies to A-F, bar in H = 20 μm and applies to G-H.

Figure 11

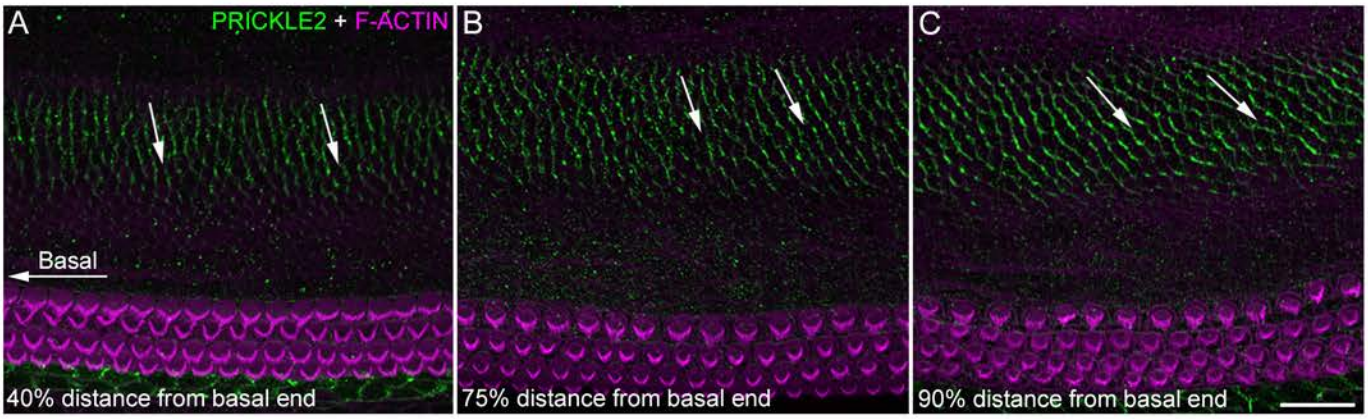

Figure 11. **PRICKLE2 distribution in underlying epithelium.** PRICKLE2 staining (green) within the GER of a P2 wild-type mouse at regions 40% (A), 75% (B) and 90% (C) from the base of the cochlea. F-ACTIN labelling is shown in red. PRICKLE2 is asymmetrically distributed around the apical pole of cells located in a narrow band within the GER, generating lines of staining that run in a medio-lateral direction with a slant that progressively increases towards the apex of the cochlea (compare orientation of arrows in A, B and C). Bar = 20 μm.

Figure 12

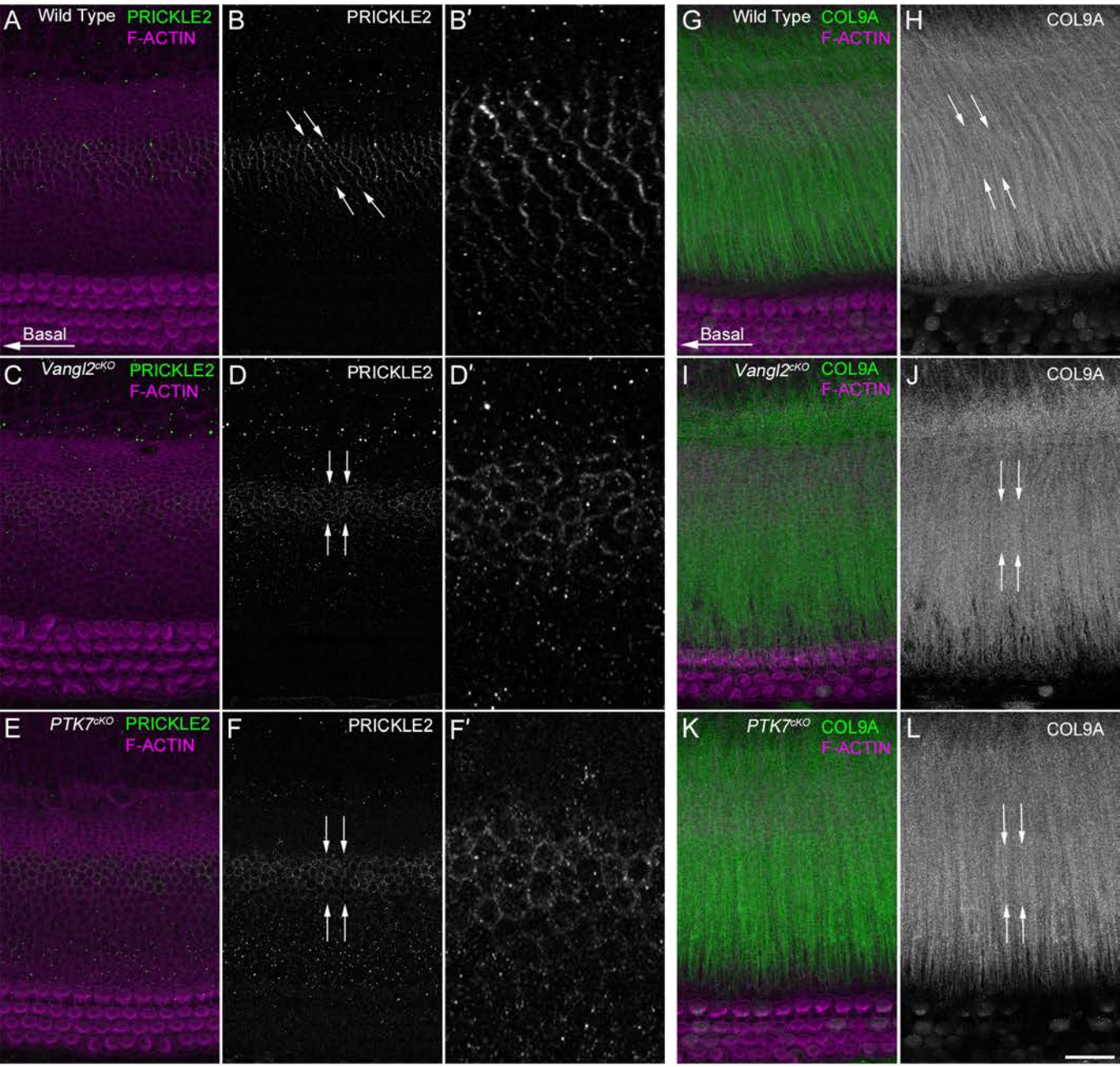

Figure 12. **PRICKLE2 distribution in *Vangl2*^{CKO} and *PTK7*^{CKO} mice**. Equivalent mid-coil regions of P1 cochleae double labelled for PRICKLE2 and F-ACTIN (A-F), or COL9A and F-ACTIN (G-L), from control (A-B, G-H), *Vangl2*^{CKO} (C-D, I-J) and *PTK7*^{CKO} (E-F, K-L) mice. PRICKLE2 staining is asymmetrically distributed within a longitudinal stripe within the GER in control animals (A-B') but not in *Vangl2*^{CKO} (C-D') or *PTK7*^{CKO} (E-F') mutants. B', D' and F' show x3 enlargements of PRICKLE2 staining shown in B, D and F respectively. In wild-type mice collagen-fibril bundles have an apically-directed slant (G-H). In the *Vangl2*^{CKO} (I-J) and *PTK7*^{CKO} (K-L) mutant mice collagen-fibril bundles are oriented in an almost perfectly radial fashion. Bar = 20 μm.

Figure 13

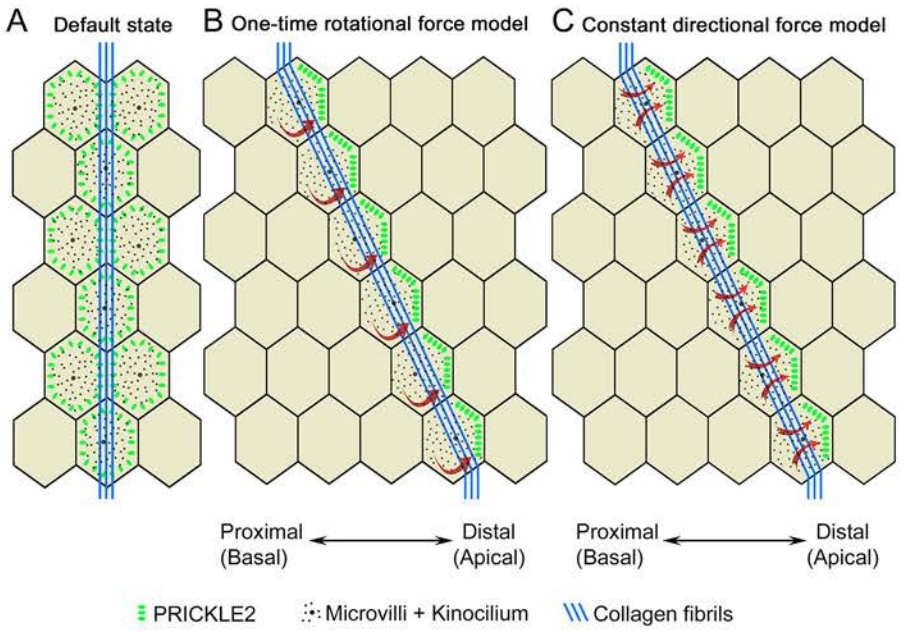

Figure 13. **Proposed models.** Two potential models (B, C) for generating apically-offset collagen-fibril bundles. A) Default state, in which collagen fibrils have a purely radial orientation. B) A one-time, PRICKLE2-dependent, actomyosin-generated rotational force reorients collagen fibrils, with subsequently produced fibrils also having a similar orientation due to templating. C) A constant, actomyosin-generated force towards the distally-localised PRICKLE2 results in collagen fibrils adopting an apical slant as they are produced. Forces are assumed to be transmitted from the junctions to the collagen fibrils via the microvilli on the surfaces of the GER cells.

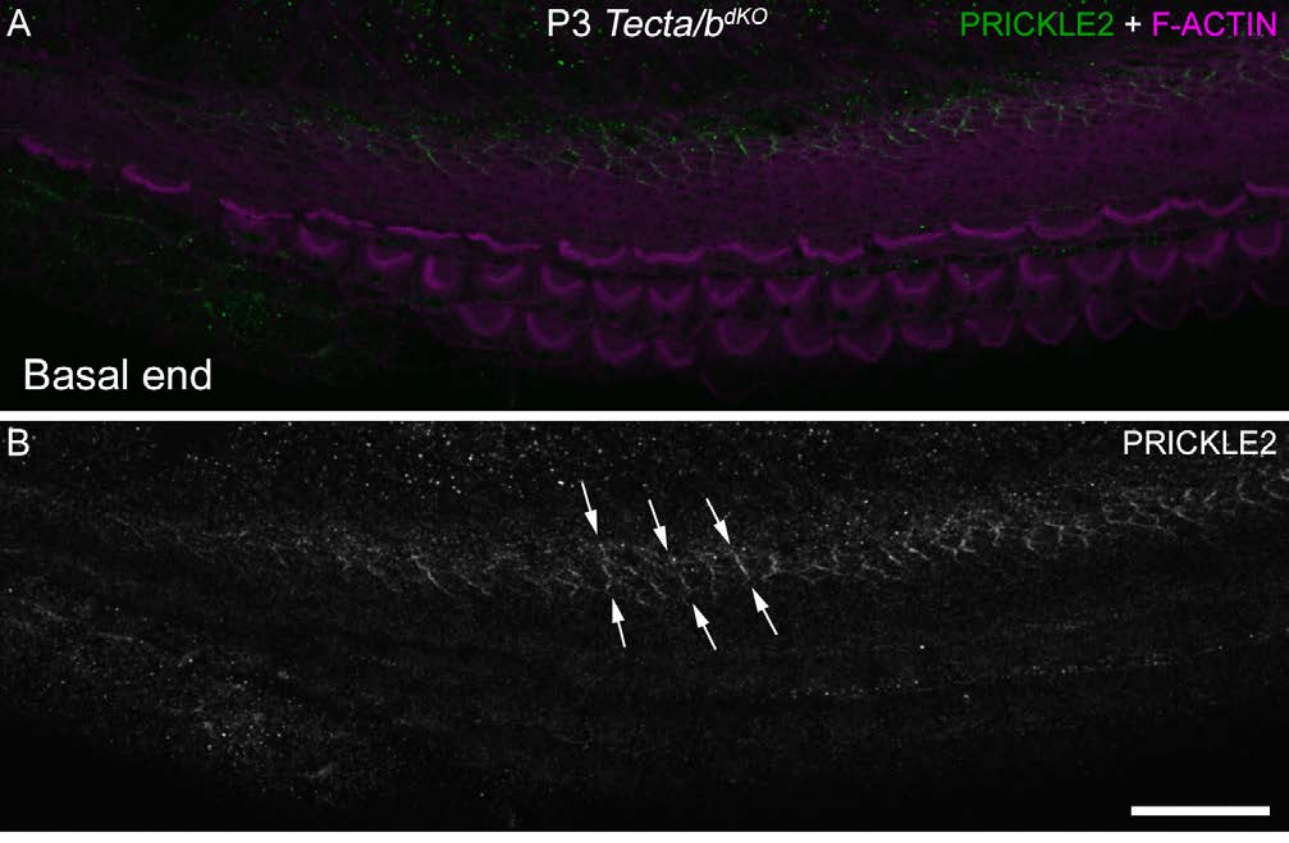

Figure S1. **PRICKLE2 distribution in *Tecta/b*^{dKO} mice**. Basal end of a P3 *Tecta/b*^{dKO} cochlea stained with antibodies to PRICKLE2 and with phalloidin. Pairs of arrows indicate that PRICKLE2 staining maintains an apically directed slant in the mutant. Bar = 20 μm.

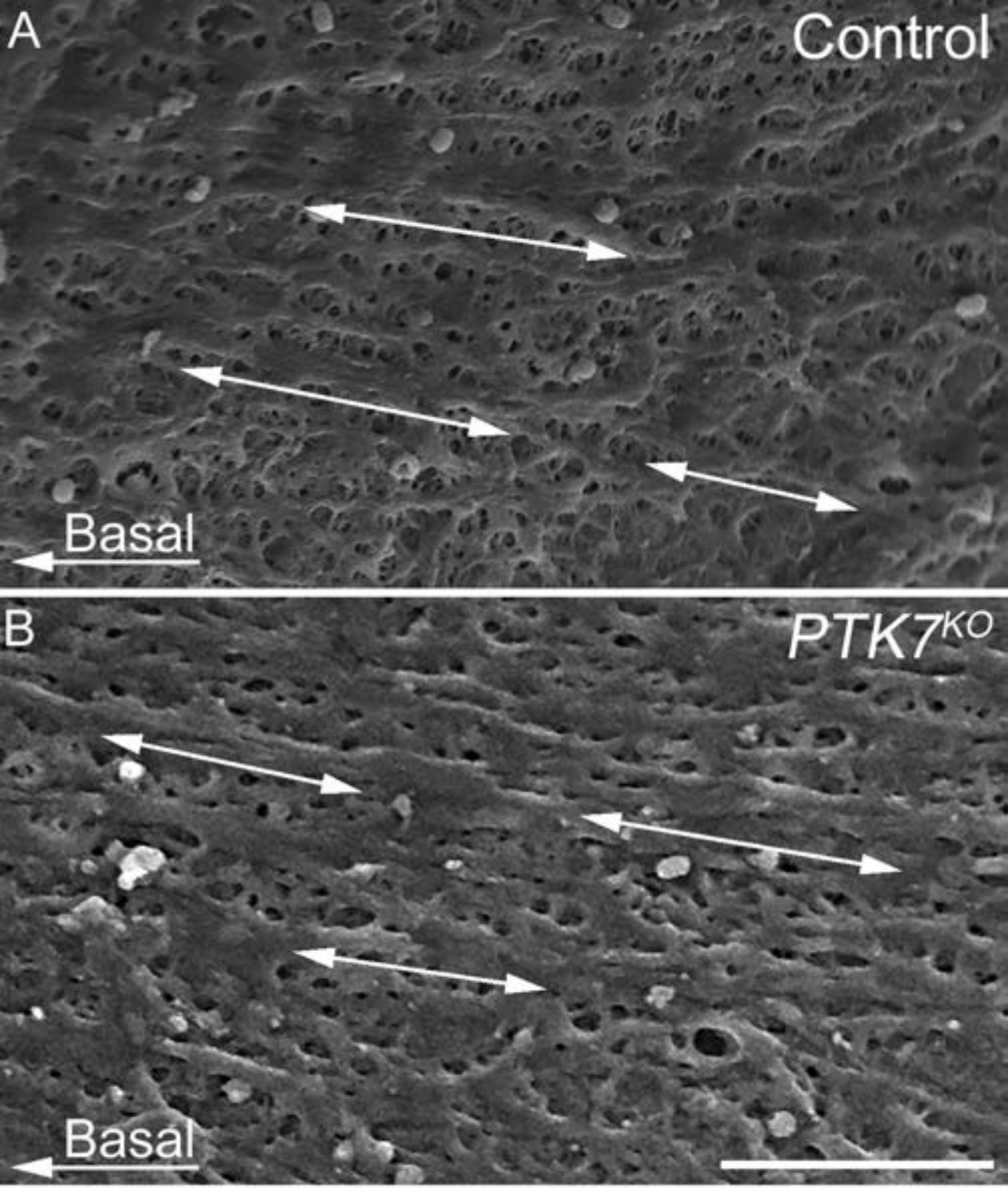

Figure S2. **TM surface features in PCP mutant.** Scanning electron micrographs showing the surface of the TM in the basal coil at E16.5 in control and *PTK7*^{KO} mice. Surface fibrils run in a broadly longitudinal direction in controls and mutants (double arrowheads). Bar = 5 μm.

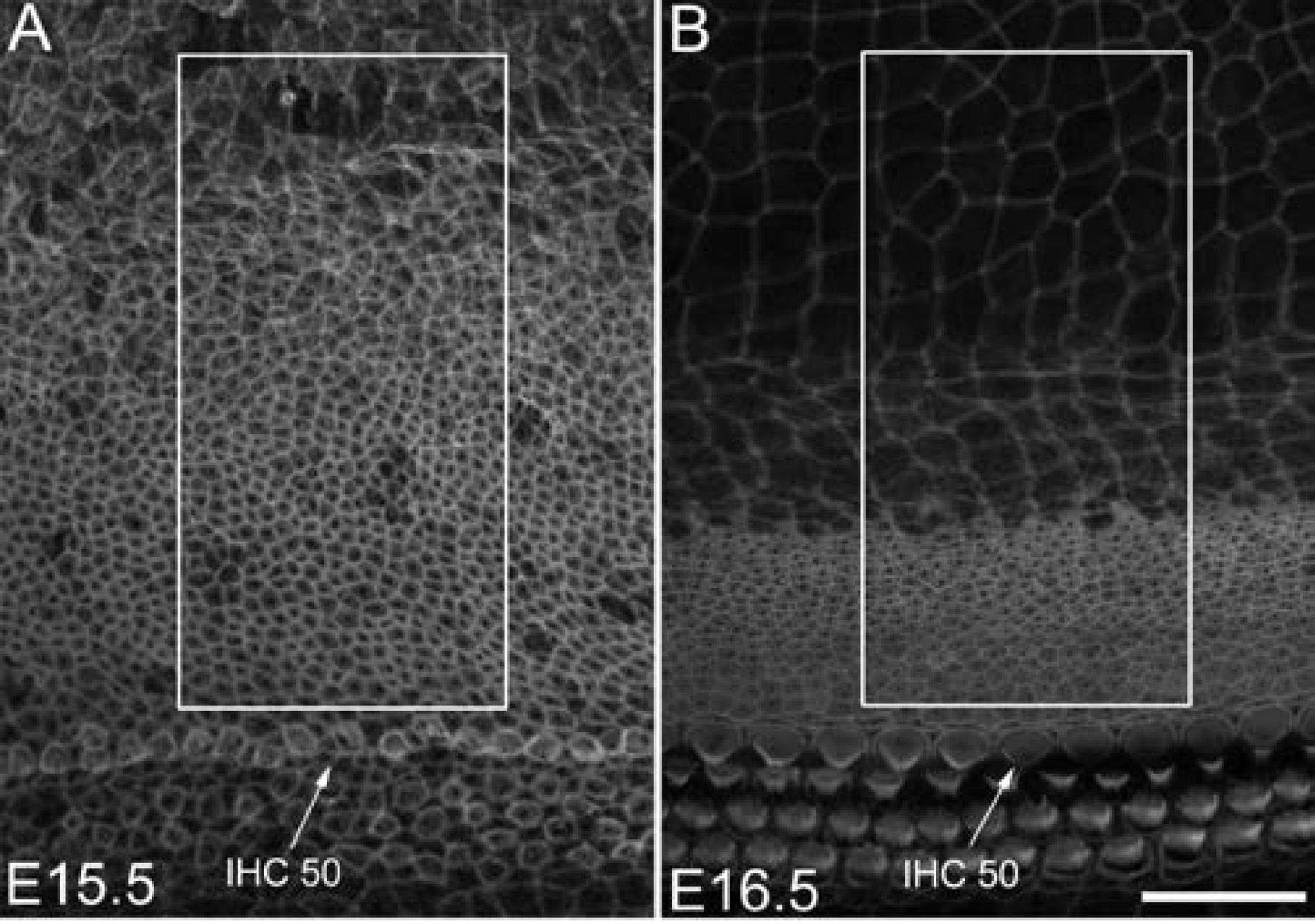

Figure S3. Phalloidin stained cochleae at E15.5 and E16.5 showing boxed, 50x100 µm GER regions selected at a distance 50 IHCs from the basal end. Apical surface numbers changed from 504 (n=5, SD=64.5) at E15.5, to 298 (n=5, SD=13.6) at E16.5, per boxed region, a statistically significant reduction ($P<0.001$, Student's t-test, two-tailed). n refers to individual cochleae from different animals. Bar = 25 µm.